# Realized Illiquidity*

Demetrio Lacava † Angelo Ranaldo‡ Paolo Santucci de Magistris §

November 21, 2022

**Abstract**

We study the theoretical and empirical properties of a simple measure of market illiquidity, namely the *realized Amihud*, which is defined as the ratio between the realized volatility and trading volume and which refines the popular price impact measure proposed by Amihud (2002). In our model, both price volatility, $\sigma(t)$, and market liquidity, $\lambda(t)$, are assumed to follow stochastic processes in continuous time. In this setting, characterized by stochastic volatility and liquidity, we prove that the realized Amihud provides a precise measurement of the inverse of *integrated liquidity*, that is, the integral of $\int_0^1 \lambda(s)\, ds$ over fixed-length periods (e.g., a day, a week, a month). We consider a number of alternative econometric specifications, hence highlighting the main dynamic and distributional properties of the realized Amihud, including jumps, clustering, and leverage effects.

**Keywords:** Liquidity, Stochastic Volatility, Trading Volume, Amihud, Jumps.

*J.E.L. classification*: C15, F31, G12, G15

*We are grateful to Tim Bollerslev, Nicola Borri, Massimiliano Caporin, Alessandro Casini, Leopoldo Catania, Dobrislav Dobrev, Deniz Erdemlioglu, Mark Hallin, Mark Podolskij, Anders Rahbek, Eduardo Rossi, Francesco Sangiorgi, and Pierluigi Vallarino for their relevant comments about our work. We thank Kim Christensen for having shared with us the realized volatility series of SPY. We also thank the participants at the Vieco conference (Copenhagen University, 2022), IAAE conference (King's College, 2022), SoFiE conference (Cambridge, 2022), Rome-Waseda Time Series Symposium (Rome, 2022), and the seminar participants at University of Pavia, at Luiss University and at IESEG School of Management. Angelo Ranaldo acknowledges financial support from the Swiss National Science Foundation (SNSF grant 182303). Paolo Santucci de Magistris also acknowledges the research support of the Project 2 grant of the Danish Council for Independent Research (IRFD), Social Sciences, number 8019-00015A.

†LUISS "Guido Carli" University, Department of Economics and Finance, Viale Romania 32, 00197 Roma, Italy

‡University of St. Gallen and Swiss Finance Institute, Switzerland. angelo.ranaldo@unisg.ch

§LUISS "Guido Carli" University, Department of Economics and Finance, Viale Romania 32, 00197 Roma, Italy; CREATES, Department of Economics and Business Economics, Aarhus University, Denmark. sdemagistris@luiss.it

# 1 Introduction

In addition to being crucial to the quality of financial markets and resilience of the financial system, market liquidity is important for capital market efficiency because "liquidity of investment markets often facilitates, though it sometimes impedes, the course of new investment" (Keynes, 1936, p.102). However, market liquidity is an elusive concept because it includes everything that determines "the degree to which an order can be executed within a short time frame at a price close to the security's consensus value" (Foucault et al., 2013, p.2). Thus, liquidity manifests itself in at least two important ways: the transaction cost and the impact of transaction volumes on security prices, which, in turn, depends on the market depth and price elasticity. The transaction cost is often gauged by the bid-ask spread, while a popular measure for price impact is the Amihud illiquidity measure (Amihud, 2002), which is the ratio between the daily absolute returns and trading volume.

In this paper, we study the theoretical and empirical properties of a refinement of the classic *daily Amihud*, namely the *realized Amihud*, which is defined as the ratio between a realized volatility measure and the daily trading volume. Figure 1 provides a simple illustration of the precision of the realized Amihud (black solid line) in relation to the daily Amihud (blue solid line). Although both series follow similar dynamic patterns, the daily Amihud is a much noisier proxy of the latent signal than the realized Amihud.

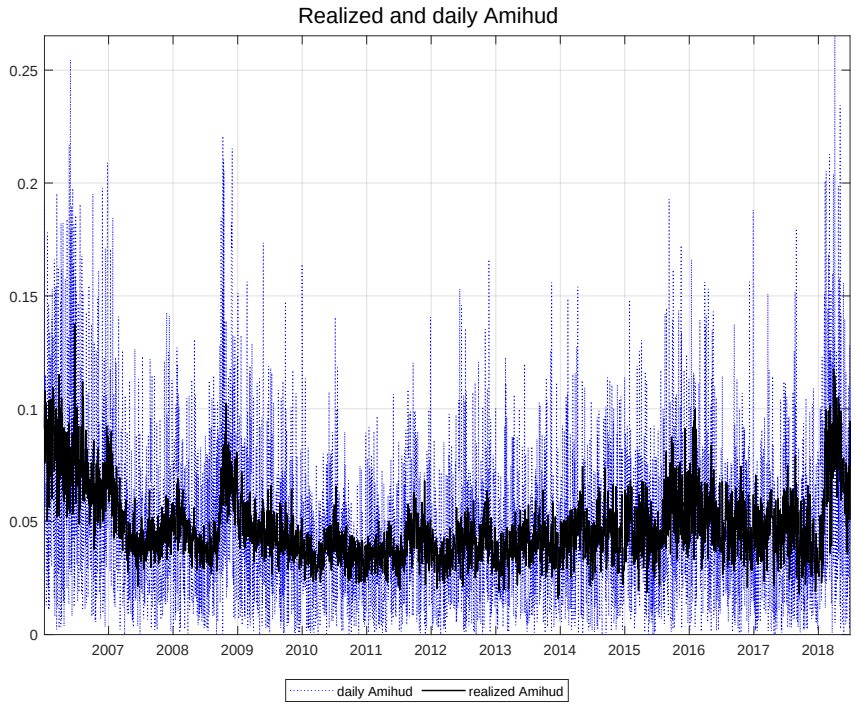


**Figure 1:** Realized Amihud (black solid line) vs daily Amihud (blue dotted line, see Amihud, 2002) of SPY. Sample period: January 3, 2006 – June 29, 2018. Both series are scaled by a factor of E+09.

This paper contributes to the literature in three ways. Our first contribution is outlining a sim-

ple theoretical framework based on the trading mechanism introduced by Clark (1973), which fits suitably into the theory of realized volatility, specifically here in the context of liquidity measurement. This allows us to construct a simple framework to formally define a stochastic quantity, namely the *integrated illiquidity*, which is the object of interest when employing the realized Amihud. Hence, we can establish *how precisely* the integrated illiquidity is measured vis-a-vis the classic daily Amihud. In developing the theory behind the realized Amihud, we consider a setting where both spot volatility, $\sigma(t)$, and the instantaneous liquidity parameter, $\lambda(t)$, are (possibly correlated) continuous-time stochastic processes. We prove that the realized Amihud provides a precise measurement of the integrated illiquidity, which is defined as the reciprocal of $\int_0^1 \lambda(s)ds$ over periods of unit length (e.g., a day, a week, or a month). Thanks to its intrinsic nonparametric nature, the realized Amihud represents a simple measure of market resiliency, that is, the elasticity of asset prices to trading volume, where the latter depends on the degree of disagreement in the beliefs among traders.

A set of Monte Carlo simulations illustrates the finite sample accuracy of the realized Amihud as a nonparametric measurement of integrated illiquidity, showing that sampling returns at 5-minute frequencies normally reduces the contamination coming from microstructural frictions stemming from other dimensions of illiquidity, such as the bid-ask spread or price staleness. In the Monte Carlo simulations, we also explore the finite-sample properties of an alternative low-frequency version of the classic daily Amihud, namely the *high-low Amihud*, which exploits the information on volatility obtained by the daily range estimator of Parkinson (1980). The range is simply based on the difference of two values, which can be easily obtained for many financial securities, even on a daily basis: the highest and lowest price achieved by the financial security during a given period. We show that the high-low Amihud provides estimates of the underlying illiquidity process that are several times more precise than those obtained by the daily Amihud. For this reason, the high-low Amihud can be considered a more efficient low-frequency alternative to the daily Amihud.

Our second contribution is to derive a simple theory for *jumps* in illiquidity, which are generated by impactful news common to all traders such as earnings press releases for stocks or central bank announcements for currencies. The natural interpretation of such jumps is the consensual price change induced by new fundamental information for which little or no transaction volume is needed to achieve it. We refer to them as *information jumps*. These events induce large volatility but little to no volume, thus mechanically increasing the observed market illiquidity. Building on the results of Barndorff-Nielsen and Shephard (2003, 2004, 2006), we develop a formal way to carry out nonparametric statistical inference on *information jumps* and disentangle the illiquidity generated by information jumps from the baseline illiquidity associated with disagreement among traders, which is the main driver of trading volume. In particular, we construct a test statistic to detect significant jumps, and we construct the jump-robust version of the realized Amihud estimator of illiquidity.

Our third contribution is to empirically study the properties of the realized Amihud. To do so, we consider a comprehensive set of alternative econometric specifications with the goal of char-

acterizing the main dynamic and distributional properties of the realized Amihud. These models are inspired by those that are usually adopted in the context of volatility modeling. In particular, we explore the (pseudo) long-memory features of the realized Amihud by estimating the heterogeneous autoregressive specification (HAR) model of Corsi (2009) in both a linear and nonlinear context. Also, we consider a multiplicative error model (MEM) specification (Engle and Gallo, 2006) that allows for a direct prediction of illiquidity without resorting to nonlinear transformations to preserve positivity. The empirical analysis, which is based on the time series of the daily realized Amihud of the main exchange traded fund (ETF) tracking the S&P 500 index (SPY), reveals a number of interesting and novel empirical features, shedding new light on the stochastic features of illiquidity. Two main findings stand out that, reminiscent of two key terms used in the volatility literature, we call *illiquidity clustering* and *leverage effect*. First, the empirical evidence strongly suggests that the latent illiquidity process is a very persistent one that is characterized by long periods of high illiquidity followed by long periods of low illiquidity. Second, when regressing excess returns on the realized Amihud, we find that illiquidity negatively correlates with stock returns at daily, weekly, and monthly frequencies, a phenomenon that we call *illiquidity leverage*. After breaking down illiquidity in its expected and unexpected components, we find that it is the unexpected part of illiquidity that is most correlated with returns. Note that both the illiquidity clustering and leverage effects are much less evident when the noisy classic daily Amihud is employed, hence reiterating the importance of using a more precise illiquidity measure, such as the realized Amihud.

Finally, we show that, despite its simplicity, our theory lends itself to several extensions that succeed in explaining the financial markets' behavior in reaction to major events such as the cap removal of EUR/CHF on January 15, 2015. The theory prescribes that the observed illiquidity would increase after the cap removal because the Swiss National Bank ceased to supply Swiss francs in unlimited quantities, thus reducing the supply of extra trading volume to the market. By carrying out the break analysis of Bai and Perron (1998), we find strong evidence that illiquidity significantly increased after January 15, 2015, as a joint consequence of an increase in EUR/CHF volatility and a reduction in trading volume of the same currency pair. Notably, we find an analogous pattern on the USD/CHF rate, suggesting that a liquidity shock in one market (or FX rate) immediately spills over into another one.

Our paper adds to prior research on market liquidity by highlighting the main theoretical and empirical properties of the realized Amihud measure. The literature in this field proposes several measures of the trading impact on security prices. Ideally, to measure this, one would need access to data on all orders submitted by traders in a centralized market. However, many markets are decentralized and opaque, such as all the over-the-counter (OTC) markets, including the FX market that we also study here. In this context, the Amihud measure is extremely useful for approximating the trading impact on security prices at the aggregate level. Kyle (1985) provides an insightful theoretical framework to explain how orders impact asset prices, as captured by his *lambda* factor. Relying only on daily price and volume data, much more accessible than tick-by-tick orders and transactions, the ILLIQ proxy proposed by Amihud (2002) offers a very practical

measure to approximate Kyle's lambda, which is easy to calculate and accurate when compared with benchmark measures such as the effective spread and order flow price impact.[1] Ranaldo and Santucci de Magistris (2022) introduce the realized Amihud to empirically study the price impact in the global FX market. We extend their work (i) by providing a theoretical foundation to the realized Amihud, (ii) by introducing the notion of integrated illiquidity, and (iii) by studying the appropriate econometric modeling that highlights its empirical features, including illiquidity jumps, clustering, and leverage effects. Our work shares similarities with that of Collin-Dufresne and Fos (2016), who extends the theoretical setting of Kyle (1985) by letting price impact and price volatility both be stochastic. Compared with Collin-Dufresne and Fos (2016), our theory is simpler but offers new insights into Amihud's measure: in a market populated by traders with different reservation prices, the realized Amihud measures the inverse of the *integrated liquidity*. Furthermore, our contribution is both on the methodological side and on the econometric side. On the methodological side, we propose an easy-to-compute measure of trading price impact that relies on the ratio between two observable quantities based on transaction data, namely the (realized) volatility and volume. In doing so, we extend the previous literature on low-frequency liquidity measures predominantly based on the estimation of bid-ask spread approximation.[2]

This present paper is organized as follows: Section 2 outlines the theoretical setting. Section 3 reports the results of several Monte Carlo simulations. Section 4 introduces the notion of information jumps and of the jump-robust realized Amihud. Section 5 presents the empirical analysis, while Section 6 concludes the paper. Proof and additional empirical results are in the Appendix.

## 2 A Simple Theory of Illiquidity Measurement

Let us consider a world in which there is a traded asset. We assume that the market consists of a finite number $J \geq 2$ of active participants who trade on the asset. Within a given trading period of a certain unit length (e.g., an hour, a day, a week), the market passes through a sequence of $i = 1, \dots I$ equilibria. The evolution of the equilibrium price is motivated by the arrival of new information to the market. At intraperiod $i$, the desired position of the $j$-th trader ($j = 1, \dots, J$) is given by

$$q_{i,j} = \lambda_i (p^*_{i,j} - p_i), \quad \lambda_i > 0, \tag{1}$$

where $p^*_{i,j}$ is the reservation price of the $j$-th trader and $p_i$ is the current market price (both measured in logs). The equilibrium function in (1) is analogous to the theory of Clark (1973) and Tauchen and Pitts (1983), which provides a stylized representation of the supply-demand mechanism on the market at the intraday level.[3] The reservation price of each trader might reflect some of the following aspects: individual preferences, liquidity issues, asymmetries in information sets,

[1] For instance, Hasbrouck (2009) provides evidence on the accuracy of the Amihud measure for stocks while Ranaldo and Santucci de Magistris (2022) does so for FX rates.

[2] Starting from the seminal work of Roll (1984), several papers propose other measures that estimate the bid-ask spread, including Hasbrouck (2009), Corwin and Schultz (2012), and Abdi and Ranaldo (2017).

[3] See also the survey in Karpoff (1987) and the empirical analysis in Andersen (1996).

and different expectations about the fundamental values of the asset. In general, the reservation price can deviate from the market price because of idiosyncratic reasons, inducing the $j$-th trader to trade. The quantity exchanged for a unit change of $p^*_{i,j} - p_i$ is given by the slope $\lambda_i$. The term $\lambda_i$ is a positive coefficient capturing the market depth at time $i$: The larger the $\lambda_i$, the larger quantities of the asset can be exchanged for a given difference $p^*_{i,j} - p_i$. In other words, $\lambda_i$ measures the capacity of the market to allow large quantities to be exchanged at the intersection between demand and supply, thus recalling the concept of market depth and resilience that reduces the price impact of trading. The baseline assumptions of the model (linearity of the trading function and constant number of active traders) are inevitably stylized. As for the form of the equilibrium function in (1), note that the trades take place on short intraday intervals of length $\delta = 1/I$ and are generally associated with small price variations. Therefore, it is not restrictive to assume the equilibrium function is linear on small price changes and for a fixed number of traders during such a short period.

By market clearing, that is $\sum_j q_{i,j} = 0$, we have that the average of the reservation prices clears the market, that is, $p_i = \frac{1}{J}\sum_{j=1}^{J} p^*_{i,j}$, and the log-return is $r_i := \Delta p_i = p_i - p_{i-1}$. Furthermore, as new information arrives, the traders adjust their reservation prices $\Delta p^*_{i,j}$, resulting in a change in the market price, which is given by the average of the increments of the reservation prices. Consequently, the generated trading volume in each $i$-th subinterval is as follows:

$$v_i = \frac{\lambda_i}{2}\sum_{j=1}^{J} |\Delta p^*_{i,j} - \Delta p_i|,$$

where $\Delta p^*_{i,j} = p^*_{i,j} - p^*_{i-1,j}$. We assume the following dynamics for the reservation prices

$$dp^*_j(t) = \mu_j(t)dt + \sigma_j(t)dW_j(t), \quad j = 1, \dots, J, \tag{2}$$

where $\{W_j(t), j = 1, \dots J\}$ is a collection of independent Wiener processes. The term $\mu_j(t)$ is a predictable process with finite variations that might represent the long-term expectation of the $j$-th trader about the asset and could be a function of fundamental quantities, such as interest rates and macroeconomic variables. The term $\sigma_j(t)$ is the stochastic (spot) volatility process of the $j$-th trader. By letting $\sigma_j$ vary across traders, we introduce heterogeneity among them. This reconciles with many realistic features, including the evidence of long-term memory in volatility, as obtained by the superposition of traders operating at different frequencies, which, for instance, can be seen with the heterogeneous autoregressive models of Müller et al. (1997) and Corsi (2009). We assume that $\sigma_j(t) > 0$ is càdlàg with (almost surely) square integrable sample paths $\forall j = 1, \dots, J$. Analogously, $\lambda(t)$ is assumed to evolve over time as a strictly positive càdlàg stochastic process. This setup is coherent, with a representation of a frictionless market where each trader participates through its reservation price to determine a new equilibrium price by carrying new information.

Consider an interval of unit length, for example, an hour, a day, or a month. For ease of exposition and tractability, we assume that trades happen on an equally spaced and uniform grid,

$i = 1, 2, \ldots I$. On the $i$-th discrete subinterval of length $\delta = \frac{1}{I}$, we have the following:

$$p^*_{i,j} = \int_{\delta(i-1)}^{\delta i} \mu_j(s)ds + \int_{\delta(i-1)}^{\delta i} \sigma_j(s)dW_j(s). \tag{3}$$

Following Barndorff-Nielsen and Shephard (2003), for a given $\delta > 0$, we can define the *realized power variation* of order one (or realized absolute variation) as $RPV = \sum_{i=1}^{I} |r_i|$. Hence, analogously to the illiquidity proxy in Amihud (2002), we can define the continuous-time version of the Amihud illiquidity measure, namely the *realized Amihud*, as follows:

$$\mathcal{A} := \frac{RPV}{v}. \tag{4}$$

This quantity gauges the price impact of trading, that is, the amount of volatility on a unit interval (as measured by $RPV$) associated with the trading "dollar" volume $v = \sum_{i=1}^{I} v_i$ generated in the same period. In other words, $\mathcal{A}$ measures the amount of volatility associated with a unit of trading volume.[4] In the model of Clark (1973), Epps and Epps (1976), and Tauchen and Pitts (1983) volatility and trading volume (often used as a proxy for liquidity) are equilibrium outcomes of information impact and are jointly related to an unobservable dynamic information flow variable. By taking the ratio between volatility and volume, we decouple the information about market illiquidity from that of the information flow.

The following proposition highlights the main determinants of realized Amihud as an illiquidity measure.

**Proposition 1.** *Consider the illiquidity measure defined in (4), the equilibrium relation in (1), and the diffusive process for reservation prices in (2). Assume that $\sigma_j(t)$ and $\lambda(t)$ are strictly positive càdlàg processes with (almost surely) square integrable sample paths $\forall j = 1, \ldots, J$. Assume $J = 2$ active traders, as representative of the two aggregated sides of the market. As $I \to \infty$ (i.e., $\delta \to 0$)*

$$p \lim_{I \to \infty} \mathcal{A} = \frac{1}{\mathcal{L}}, \tag{5}$$

*Furthermore, as $I \to \infty$*

$$\frac{\log(\mathcal{A}) - \log\left(\frac{1}{\mathcal{L}}\right)}{\sqrt{\frac{2\delta(\pi/2-1)RV}{(\pi\delta/2)RPV^2}}} \xrightarrow{d} N(0,1), \tag{6}$$

*where $RV = \sum_{i=1}^{I} r_i^2$ is the realized variance.*

*Proof.* Proof in Appendix A.1. □

Proposition 1 shows that the realized Amihud is a measure of the reciprocal of the daily integrated liquidity $\mathcal{L}$, namely the *integrated illiquidity*, and the precision of the measurement increases as $I$ increases. Furthermore, the asymptotic distribution in (6) can be used to construct a

[4] Alternatively, one could employ the *Amivest*, which is defined as the reciprocal of Amihud, that is, as the ratio of volume over volatility.

confidence interval for $\mathcal{L}$. In the next section, we run Monte Carlo simulations to assess the finite sample performance of the realized Amihud in measuring illiquidity.

# 3 Monte Carlo Simulations

Resorting to the continuous-time framework outlined in Barndorff-Nielsen and Shephard (2002a,b), we can precisely measure the variability of the asset price by computing RPV over intervals of any length (e.g., hours, days, weeks, and months). Furthermore, the equilibrium theory presented above allows us to relate this variability to the aggregate level of disagreement among investors, in turn leading to the observed trading volume. An assessment of the quality of the measurement of illiquidity based on the realized Amihud is carried out by Monte Carlo simulations. The liquidity process, $\lambda(t)$, is generated according to a Heston-type SDF:

$$d\lambda(t) = \kappa_\lambda(\lambda(t) - \lambda_0)dt + \eta_\lambda \lambda(t)^{1/2} dW_\lambda(t),$$

where $\lambda_0 = 50, 200, 500$ represents the long-term mean in the low-, medium-, and high-liquidity scenarios, respectively. The parameters $\kappa_\lambda = 0.5$ and $\eta_\lambda = 0.1$ determine the speed of the mean-reversion and the volatility of liquidity, respectively. Similarly, also the reservation prices (and, hence, equilibrium prices) is generated according to the diffusive process in (2), where the variance, $\sigma_j^2(t)$ with $j = 1, 2$, evolves following the dynamics of the Heston model, that is, $d\sigma_j^2(t) = \kappa_\sigma(\sigma^2(t) - \sigma_0^2)dt + \eta_\sigma \sigma(t) dW_{\sigma,j}(t)$ with the parameters $\kappa_\sigma = 0.2$, $\sigma_0^2 = 2$, $\eta_\sigma = 0.1$.[5] In the simulation of price and volume trajectories, we consider $T = 1,000$ transaction days and $I^* = 5,760$ intradaily intervals corresponding to a 15-second frequency over 24 hours. The RPV is then computed aggregating absolute returns sampled at different frequencies: 1 hour; 30, 15, 10, 5 minutes; and 30 and 15 seconds, that is, $I = [24, 48, 96, 144, 288, 1440, 2880, 5760]$ subintervals, respectively.

As a graphical illustration of the ability of the realized Amihud to precisely measure the latent illiquidity process, the four graphs to the left of Figure 2 report the true liquidity signal (in red), together with its estimates obtained with the realized Amihud sampling at different frequencies (blue dots). As the sampling frequency increases, the variability around the true illiquidity signal decreases, and it becomes negligible at the 1-minute frequency. In other words, by taking the ratio between a increasingly refined (in $I$) measurement of daily volatility and daily trading volume, we can obtain a very precise measurement of the day-by-day variations of the trade impact, which is a relevant dimension of illiquidity. The graph to the right of Figure 2 confirms the accuracy of the realized Amihud to capture the latent illiquidity process by showing the 95% confidence bands. More precisely, we exploit the asymptotic distribution result in Proposition 1 and report the 95% confidence bands around the true (log) illiquidity signal, $\log \mathcal{L}$, which is based on the realized Amihud computed with 1-minute returns. As clearly observable, the true illiquidity series lies within the confidence bands, thus confirming in finite samples the validity of the asymptotic

[5] The configuration of these parameters generates a persistent volatility process with daily percentage returns typically ranging in the interval between -3% and +3%. In line with the empirical evidence displayed in Section 5, the simulated liquidity process $\lambda(t)$ also displays a persistent behavior.

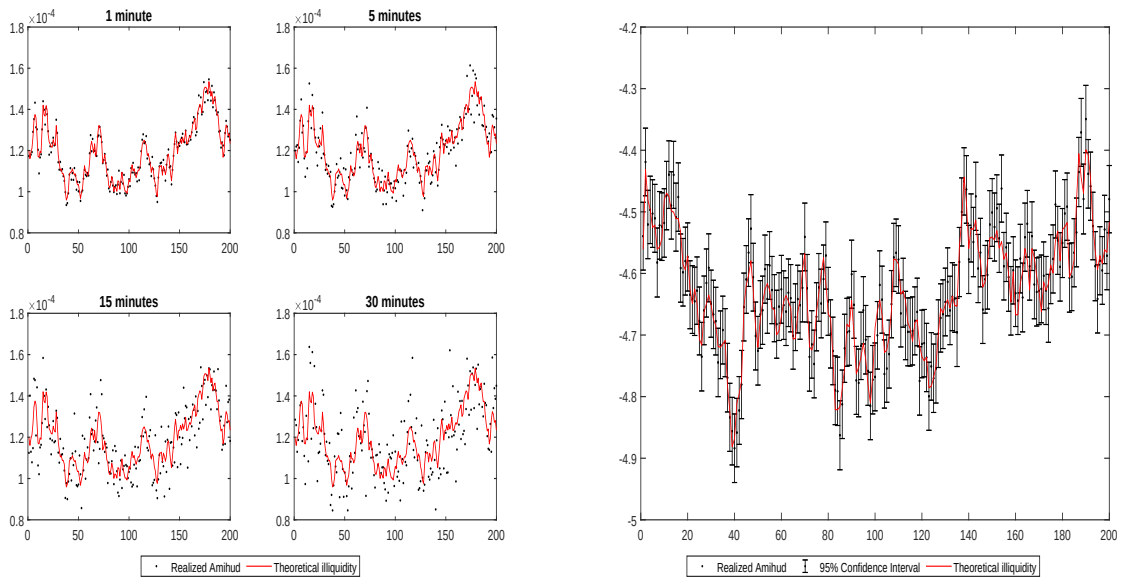


**Figure 2:** The realized Amihud at different frequencies and confidence intervals. The four figures on the left report the true illiquidity limit $\frac{1}{\mathcal{L}}$ (red solid line), and the realized Amihud (dots) obtained sampling returns at different frequencies of 1 minute, 5, 15 and 30 minutes for $T = 200$ days. The figure on the right reports the true illiquidity signal (log $\mathcal{L}$, red) and 95% confidence bands based on the realized Amihud computed with 1-minute returns.

result in Proposition 1. Thus, the main message that arises from this analysis and Figure 2 is that, in a frictionless market, the higher the sampling frequency is, the better the approximation will be. Arguably, this result can drastically change when considering microstructure frictions (in the form of bid-ask spreads and price discreetness). We will address this question in Section 3.1 below. As a further illustration to assess the finite-sample performance of the asymptotic distributions of the realized Amihud, we construct quantile-quantile (QQ-) plots based on equation (22). Figure 3 reports the QQ-plots based on the simulation experiment described above, where $I = 24, 76, 288, 1440$. As $I$ increases, the fit of to the Gaussian distribution improves, and it is already remarkable at 5-minute frequencies.

The summary of the results of the Monte Carlo simulations are presented in Table 1. The realized Amihud provides accurate measurements of the true integrated illiquidity process (i.e., $\frac{1}{\mathcal{L}}$) in all scenarios (low-, medium-, and high-illiquidity levels) with a relative bias below 0.5% in absolute value and a small RMSE, even for relatively moderate sampling frequencies (e.g., 5-10 minutes). As expected from Theorem (1), the RMSE decreases as $I$ increases (i.e., $\delta$ decreases). In general the RMSE of the realized Amihud is much smaller compared with the RMSE achieved by the daily Amihud. The latter can be considered an extreme case of illiquidity measurement obtained with only one observation per trading period, that is, $I = \delta = 1$. In this case, the illiquidity measure in (4) reduces to $\mathcal{A}^D = \frac{|r|}{v}$.

We also consider an alternative low-frequency version of the daily Amihud, that is, the high-low Amihud that is obtained by exploiting the high-low price range as a proxy of volatility, see

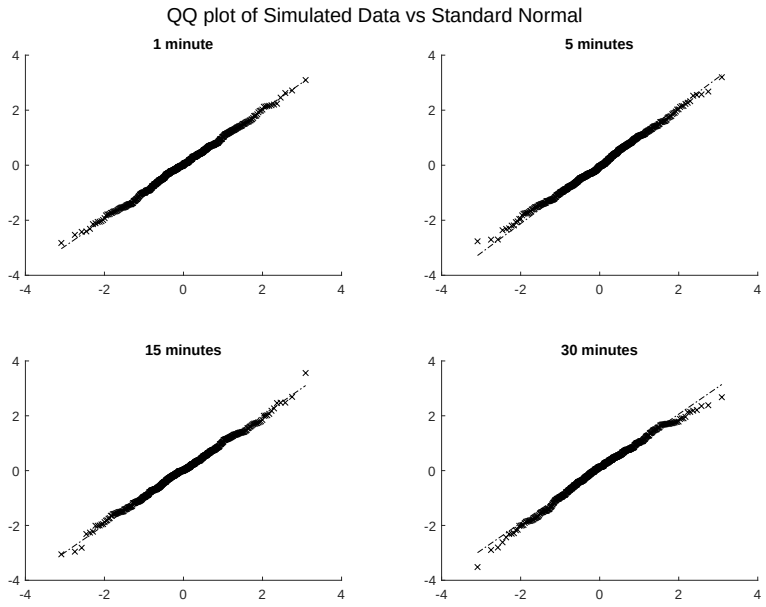


**Figure 3:** QQ-plot. Figure reports the QQ-plots and illustrates the approximation of $\frac{\log(\mathcal{A})-\log\left(\frac{1}{L}\right)}{\sqrt{\frac{2\delta(\pi/2-1)RV}{(\pi\delta/2)RPV^2}}}$ to a standard Gaussian random variable as in (6). We consider different sampling frequencies, namely 1 minute, 5 and 15 minutes, and 1 hour.

Parkinson (1980), among others. In particular, the high-low Amihud is defined as $\mathcal{A}^{HL} = \frac{range}{v}$, where $range = \sqrt{\frac{1}{4\log(2)}(p_t^H - p_t^L)^2}$ with $p_t^H$ and $p_t^L$ being the daily high and low log-prices, respectively. The Monte Carlo simulations show that the high-low Amihud displays remarkable properties. It is characterized by a small negative bias (around 5%) and is approximately three times more efficient than the traditional daily Amihud. This suggests that the high-low Amihud constitutes a viable alternative to the daily Amihud when when prices are available at low frequency only.

## 3.1 Microstructure Frictions

It should be stressed that the asymptotic results (in the limit for $I \to \infty$) behind Proposition 1 are derived by abstracting them from microstructure frictions (namely *microstructure noise*), like transaction costs in the form of bid-ask spread, clearing fees, or price discreteness, which are intimately related and endogenous to the trading process.

In the simplified context provided by the model, the microstructure features linked to the actual cost of trading (which is another dimension of illiquidity) in the form of a bid-ask spread are not explicitly included, but they pose a relevant empirical issue. From a statistical point of view, the microstructure noise dominates the volatility signal as $I \to \infty$, thus leading to distorted measurements of the variance. In the literature on realized variance (see, among many others, Bandi and Russell, 2008; Liu et al., 2015), it is common practice to resort to moderate sampling frequencies, for example, 5-minute intervals, to reduce the impact of the microstructure noise

| **Low Liquidity**, $\lambda_0 = 50$ | | | | | | |
|---|---|---|---|---|---|---|
| | Percentage Relative Bias | | | Relative RMSE | | |
| | Realized Amihud | High-Low Amihud | Daily Amihud | Realized Amihud | High-Low Amihud | Daily Amihud |
| 1h | 1.6445 | -5.5453 | -2.5699 | 0.2330 | 0.2924 | 0.7450 |
| 30min | 0.4541 | -5.5453 | -2.5699 | 0.1504 | 0.2924 | 0.7450 |
| 15min | 0.5667 | -5.5453 | -2.5699 | 0.1097 | 0.2924 | 0.7450 |
| 10min | -0.0095 | -5.5453 | -2.5699 | 0.0901 | 0.2924 | 0.7450 |
| 5min | 0.2309 | -5.5453 | -2.5699 | 0.0614 | 0.2924 | 0.7450 |
| 1min | 0.0923 | -5.5453 | -2.5699 | 0.0291 | 0.2924 | 0.7450 |
| 30sec | 0.1065 | -5.5453 | -2.5699 | 0.0201 | 0.2924 | 0.7450 |
| 15sec | 0.0630 | -5.5453 | -2.5699 | **0.0142** | 0.2924 | 0.7450 |
| **Medium Liquidity**, $\lambda_0 = 200$ | | | | | | |
| | Percentage Relative Bias | | | Relative RMSE | | |
| | Realized Amihud | High-Low Amihud | Daily Amihud | Realized Amihud | High-Low Amihud | Daily Amihud |
| 1h | 3.6035 | -3.9223 | -2.4906 | 0.2326 | 0.2934 | 0.7547 |
| 30min | 2.2201 | -3.9223 | -2.4906 | 0.1581 | 0.2934 | 0.7547 |
| 15min | 0.5300 | -3.9223 | -2.4906 | 0.1084 | 0.2934 | 0.7547 |
| 10min | 0.6963 | -3.9223 | -2.4906 | 0.0874 | 0.2934 | 0.7547 |
| 5min | 0.2997 | -3.9223 | -2.4906 | 0.0615 | 0.2934 | 0.7547 |
| 1min | 0.0216 | -3.9223 | -2.4906 | 0.0277 | 0.2934 | 0.7547 |
| 30sec | -0.0456 | -3.9223 | -2.4906 | 0.0194 | 0.2934 | 0.7547 |
| 15sec | 0.0045 | -3.9223 | -2.4906 | **0.0139** | 0.2934 | 0.7547 |
| **High Liquidity**, $\lambda_0 = 500$ | | | | | | |
| | Percentage Relative Bias | | | Relative RMSE | | |
| | Realized Amihud | High-Low Amihud | Daily Amihud | Realized Amihud | High-Low Amihud | Daily Amihud |
| 1h | 3.1471 | -6.4177 | -4.7968 | 0.2330 | 0.2918 | 0.7575 |
| 30min | 1.6101 | -6.4177 | -4.7968 | 0.1616 | 0.2918 | 0.7575 |
| 15min | 0.8523 | -6.4177 | -4.7968 | 0.1096 | 0.2918 | 0.7575 |
| 10min | 0.6709 | -6.4177 | -4.7968 | 0.0898 | 0.2918 | 0.7575 |
| 5min | 0.2646 | -6.4177 | -4.7968 | 0.0634 | 0.2918 | 0.7575 |
| 1min | 0.0035 | -6.4177 | -4.7968 | 0.0279 | 0.2918 | 0.7575 |
| 30sec | 0.0655 | -6.4177 | -4.7968 | 0.0200 | 0.2918 | 0.7575 |
| 15sec | 0.0598 | -6.4177 | -4.7968 | **0.0146** | 0.2918 | 0.7575 |

**Table 1:** Illiquidity measurement. The table reports Monte Carlo simulations for the assessment of the quality of illiquidity through the realized Amihud. It also reports the Monte Carlo relative percentage bias and RMSE (both relative to $\frac{1}{\mathcal{L}}$) for the realized Amihud reported in (4). In bold. the smallest RMSE is given. As a reference, we also consider the daily Amihud measure, that is, $\mathcal{A}^D = \frac{|r|}{v}$, and the high-low Amihud, $\mathcal{A}^{HL} = \frac{range}{v}$, where *range* is scaled by $\sqrt{\pi/2}$ to be comparable with the *RPV*.

contamination on the volatility measurement. This approach can be carried over to the illiquidity measurement, and its effectiveness in reducing the impact of microstructure noise contamination is confirmed by the evidence reported in Table 2. In particular, we repeat the analysis of Table 1, but this time, we add the bid-ask spread to the equilibrium prices and a rounding mechanism that generates price discreetness (rounding to cents or decimalization effect) and zero returns; for more, see Bandi et al. (2020), among others. The results in Table 2 suggest that, in this setting, we should avoid computing the realized Amihud by sampling at the highest possible frequencies (e.g., from 15 to 30 seconds) because this leads to large estimation biases. Instead, sampling at moderate frequencies (e.g., from 5 to 10 minutes) drastically reduces the bias while also leading to a low RMSE, especially if compared with the daily Amihud, which is about 10 times larger (0.069 compared with 0.733 for the medium liquidity scenario). In summary, the realized Amihud based on 5-minute returns provides accurate measurements of the illiquidity associated with the price impact even in settings characterized by other dimensions of illiquidity: the transaction costs such as the bid-ask spread, and additional frictions such as staleness due to inherent price discreetness and absence of new information. In the empirical analysis below, we work assuming that sampling asset returns at 5-minute intervals is sufficient to achieve a precise measurement

| **Low Liquidity**, $\lambda_0 = 50$ | | | | | | |
|---|---|---|---|---|---|---|
| | Percentage Relative Bias | | | Relative RMSE | | |
| | Realized Amihud | High-Low Amihud | Daily Amihud | Realized Amihud | High-Low Amihud | Daily Amihud |
| 1h | 1.8020 | -4.8748 | -0.7818 | 0.2176 | 0.3054 | 0.7711 |
| 30min | 1.8298 | -4.8748 | -0.7818 | 0.1569 | 0.3054 | 0.7711 |
| 15min | 1.6781 | -4.8748 | -0.7818 | 0.1151 | 0.3054 | 0.7711 |
| 10min | 1.7789 | -4.8748 | -0.7818 | 0.0921 | 0.3054 | 0.7711 |
| 5min | 2.9765 | -4.8748 | -0.7818 | **0.0725** | 0.3054 | 0.7711 |
| 1min | 13.3029 | -4.8748 | -0.7818 | 0.1476 | 0.3054 | 0.7711 |
| 30sec | 25.1862 | -4.8748 | -0.7818 | 0.2720 | 0.3054 | 0.7711 |
| 15sec | 28.4629 | -4.8748 | -0.7818 | 0.3149 | 0.3054 | 0.7711 |
| **Medium Liquidity**, $\lambda_0 = 200$ | | | | | | |
| | Percentage Relative Bias | | | Relative RMSE | | |
| | Realized Amihud | High-Low Amihud | Daily Amihud | Realized Amihud | High-Low Amihud | Daily Amihud |
| 1h | 2.9646 | -4.8349 | -1.9522 | 0.2258 | 0.2812 | 0.7334 |
| 30min | 1.5911 | -4.8349 | -1.9522 | 0.1587 | 0.2812 | 0.7334 |
| 15min | 1.5683 | -4.8349 | -1.9522 | 0.1110 | 0.2812 | 0.7334 |
| 10min | 1.8408 | -4.8349 | -1.9522 | 0.0930 | 0.2812 | 0.7334 |
| 5min | 2.6054 | -4.8349 | -1.9522 | **0.0690** | 0.2812 | 0.7334 |
| 1min | 12.0901 | -4.8349 | -1.9522 | 0.1276 | 0.2812 | 0.7334 |
| 30sec | 22.9034 | -4.8349 | -1.9522 | 0.2355 | 0.2812 | 0.7334 |
| 15sec | 25.5046 | -4.8349 | -1.9522 | 0.2640 | 0.2812 | 0.7334 |
| **High Liquidity**, $\lambda_0 = 500$ | | | | | | |
| | Percentage Relative Bias | | | Relative RMSE | | |
| | Realized Amihud | High-Low Amihud | Daily Amihud | Realized Amihud | High-Low Amihud | Daily Amihud |
| 1h | 1.8504 | -5.9370 | -1.3766 | 0.2463 | 0.2818 | 0.7248 |
| 30min | 0.9157 | -5.9370 | -1.3766 | 0.1640 | 0.2818 | 0.7248 |
| 15min | 0.9431 | -5.9370 | -1.3766 | 0.1097 | 0.2818 | 0.7248 |
| 10min | 1.1633 | -5.9370 | -1.3766 | 0.0892 | 0.2818 | 0.7248 |
| 5min | 2.2907 | -5.9370 | -1.3766 | **0.0676** | 0.2818 | 0.7248 |
| 1min | 8.9761 | -5.9370 | -1.3766 | 0.0964 | 0.2818 | 0.7248 |
| 30sec | 16.9324 | -5.9370 | -1.3766 | 0.1736 | 0.2818 | 0.7248 |
| 15sec | 17.0739 | -5.9370 | -1.3766 | 0.1764 | 0.2818 | 0.7248 |

**Table 2:** Illiquidity measurement with microstructure noise. The table reports Monte Carlo simulations for assessing the quality of illiquidity through the realized Amihud. The bid-ask spread is set at 0.15% relative to the price level, which in line with the observed relative bis-ask spread of SPY (see Section 5). Table reports the Monte Carlo relative percentage bias and RMSE (both relative to $\frac{1}{I}$) for the realized Amihud reported in (4). In bold, the smallest RMSE is given. As a reference, we also consider the daily Amihud measure, that is, $\mathcal{A}^D = \frac{|r|}{v}$, and the high-low Amihud, $\mathcal{A}^{HL} = \frac{range}{v}$, where $range$ is scaled by $\sqrt{\pi/2}$ to be comparable with the $RPV$.

of the asset illiquidity.

# 4 Information Jumps

Now, we further explore the relationship between liquidity and volatility, focusing on the arrival of large news common to all traders. Note that the increments of the reservation log-prices can be disentangled as follows:

$$\Delta p^*_{i,j} = \phi_i + \psi_{i,j}, \quad \text{with} \quad j = 1, \dots, J,$$

where $\phi_i$ represents a fundamental information component common to all traders, stemming from public information events, such as those associated with earnings press releases or central banks' announcements. This could be related to events that trigger common directional expectations among practitioners. The term $\psi_{i,j}$ represents the investor's specific component of the reservation price, and it is assumed to follow the diffusive process in (2). Furthermore, the assumption of

independence between $\phi_i$ and $\psi_{i,j}$ across time and traders does not allow for reversal or spillover effects, such as those studied in Grossman and Miller (1988), to investigate the mechanics of liquidity provision. The same type of sequential trading behavior has been recently proven to be responsible for crash episodes, as shown in Christensen et al. (2022), and associated with changes in the level of investors' disagreement around important news announcements (see, e.g., Bollerslev et al., 2018).[6] The detection of such informational events needs an accurate identification econometric technique and granular (intraday) data. The recent advances in the literature on *jump* processes help in this analysis. Similarly to Bollerslev et al. (2018), we rely on a simple setup for the common news component, to separately identify it from the component of price variation due to the disagreement among traders, which is responsible for generating the trading volume. Other studies associating large price jumps with news announcements can be found in Andersen et al. (2007), Chaboud et al. (2008), Lee (2011), Jiang et al. (2011). For this reason, we refer to the term $\phi_i$ as *information jumps*.

In other words, when a common large news hits the market, the reservation prices all change in the same direction, thus leading to a new equilibrium price. This generates price volatility with little or no associated trading volume, so the realized Amihud is expected to be subject to a large positive shock. Ideally, we would like to disentangle this spike from the measurement of illiquidity related with the disagreement among traders. We rely upon the theory of multipower variation developed in Barndorff-Nielsen and Shephard (2003, 2004, 2006) to carry out inference on information jumps in illiquidity. Following Barndorff-Nielsen and Shephard (2006), we assume that $\phi_i$ is a compound Poisson process, namely $\phi_i = \sum_{j=1}^{\mathcal{N}_i} c_j$, where $\mathcal{N}_i$ is a simple process (e.g., a Poisson) that counts the number of jump arrivals in the interval $[i-1, i]$, and it is finite for all intervals $i$. The terms $c_j$ are nonzero random variables that determine the size of the jumps. When $\mathcal{N}_i = 0$, then $\Delta p^*_{i,j}$ reduces to the stochastic volatility plus drift model, whose dynamics are described in (2).

To carry out inference on jumps, we consider the multipower variation of order 1/2, namely

$$MPV = \frac{I}{I-1} \sum_{i=2}^{I} |r_i|^{1/2} |r_{i-1}|^{1/2}. \tag{7}$$

Following Barndorff-Nielsen and Shephard (2004, 2006), MPV converges to $\mathcal{S}$, even when $\phi_i \neq 0$, that is

$$p \lim_{I \to \infty} \delta^{1/2} \mu_{1/2}^{-2} MPV = \mathcal{S}, \tag{8}$$

where $\mu_{1/2} = E[|X|]^{1/2}$ is a normalizing constant. Therefore, we can devise the test statistic, $\mathcal{J}$, which is given by

$$\mathcal{J} = \frac{\sqrt{\pi/2}\mu_{1/2}^2 RPV - MPV}{\widetilde{BPV}}, \tag{9}$$

[6] Perraudin and Vitale (1996) also consider jump times as moments at which significant information becomes public knowledge.

where $\widetilde{BPV} = \sqrt{\xi \sum_{i=2}^{I} |r_i||r_{i-1}|}$ and $\xi = \theta(\mu_1^2 + 2\mu_{1/2}^2\mu_1 - 3\mu_{1/2}^4)/\mu_1^2)$ is a scaling constant with $\theta = 0.1032$. Under the null hypothesis that $\phi_i = 0$, $\mathcal{J} \xrightarrow{d} N(0,1)$, we can use this result for testing the presence of a significant information jump in a given day. Based on this, we can construct the *jump-robust* realized Amihud as

$$\mathcal{A}^C = \frac{RPV_C}{v}, \tag{10}$$

where $RPV_C$ is the jump-robust realized power variation, given by

$$RPV_C = \mathbb{I}(\mathcal{J} \leq q_{1-\alpha})RPV + \mathbb{I}(\mathcal{J} > q_{1-\alpha})\widetilde{MPV}, \tag{11}$$

where $\mathbb{I}(\cdot)$ is the indicator function, $q_{1-\alpha}$ denotes the $(1-\alpha)$-th quantile of a standard normal, $\alpha$ is the significance level of the jump test, and $\widetilde{MPV} = \sqrt{2/\pi}\mu_{1/2}^{-2}MPV$.

In the following, we study the finite-sample size and power properties of the $\mathcal{J}$-test by Monte Carlo simulations by considering a frictionless process (Table 3) and a process characterized by microstructure noise in the form of bid-ask spread and rounding effects (Table 4). We consider three levels of nominal size, namely $\alpha = 5\%, 1\%, 0.5\%$. In the frictionless setting, the best performance in terms of empirical size and power is achieved sampling at the highest possible frequency of 15-seconds. Furthermore, considering a setting where $\phi_i \neq 0$ allows us to study the power of the test, that is, the ability to identify a jump if it occurs. In particular, we assume that $\phi_i$ follows a compound Poisson process with an intensity equal to 5% (one jump every twenty days on average). Notably, the test correctly identifies jumps, that is, rejects the null hypothesis of no jumps, in more than 90% of the cases when sampling at the highest frequencies.

The results are quite different when considering microstructure noise. In particular, rounding to the closest cent of the dollar generates a large number of zeros in the returns sampled at the highest frequencies, as shown by Bandi et al. (2020). Kolokolov and Renò (2021) illustrate the detrimental effect of zeros on the quality of volatility estimates, especially when power variation measures are adopted. In circumstances where zeros are the dominant feature of the high-frequency returns (like for very illiquid stocks), the effect of the rounding on MPV is detrimental. In this case, MPV is associated with a large negative bias, and the jump test rejects the null hypothesis very frequently. In this case, sampling at 10 to 15 minutes frequencies drastically reduces the bias in MPV, thus leading to empirical sizes of the jump test closer to the theoretical ones. At these frequencies, the power remains high and above 85% in all cases.

# 5 Empirical Analysis

We now illustrate how the liquidity conditions of financial markets can be studied by looking at the temporal evolution of the realized Amihud. In particular, we consider the time series of the realized Amihud of SPDR S&P 500 ETF (ticker SPY), which is the ETF tracking the S&P 500 index, and of the EUR/CHF and USD/CHF foreign exchange (FX) rates. With a daily volume of 82.45 million shares in the period 2016–2021, SPY is the ETF with the largest trading volume in the

| **Low Liquidity** | Power | | | Size | | |
|---|---|---|---|---|---|---|
| | 5% | 1% | 0.5% | 5% | 1% | 0.5% |
| 1h | 79.83% | 75.35% | 73.80% | 10.31% | 4.69% | 3.52% |
| 30min | 84.71% | 80.85% | 79.55% | 8.48% | 3.16% | 2.18% |
| 15min | 86.97% | 83.54% | 82.56% | 7.68% | 2.51% | 1.56% |
| 10min | 88.83% | 85.83% | 84.40% | 6.65% | 2.02% | 1.29% |
| 5min | 90.55% | 87.55% | 86.48% | 6.25% | 1.77% | 1.10% |
| 1min | 92.67% | 90.19% | 89.16% | 5.63% | 1.35% | 0.77% |
| 30sec | 93.35% | 90.71% | 89.77% | 5.72% | 1.33% | 0.69% |
| 15sec | 93.52% | 91.45% | 90.67% | 5.44% | 1.18% | 0.63% |
| **Medium Liquidity** | Power | | | Size | | |
| | 5% | 1% | 0.5% | 5% | 1% | 0.5% |
| 1h | 79.87% | 75.46% | 73.96% | 10.70% | 4.89% | 3.69% |
| 30min | 85.06% | 81.18% | 79.60% | 8.72% | 3.42% | 2.31% |
| 15min | 87.82% | 84.48% | 83.05% | 7.07% | 2.42% | 1.54% |
| 10min | 89.16% | 86.04% | 84.94% | 6.98% | 2.29% | 1.30% |
| 5min | 90.47% | 87.56% | 86.65% | 6.53% | 1.92% | 1.05% |
| 1min | 92.86% | 90.29% | 89.55% | 5.66% | 1.24% | 0.68% |
| 30sec | 93.13% | 90.97% | 90.05% | 5.47% | 1.38% | 0.81% |
| 15sec | 93.59% | 91.15% | 90.48% | 5.77% | 1.35% | 0.73% |
| **High Liquidity** | Power | | | Size | | |
| | 5% | 1% | 0.5% | 5% | 1% | 0.5% |
| 1h | 80.24% | 76.05% | 74.22% | 10.48% | 5.10% | 4.10% |
| 30min | 84.04% | 80.22% | 78.79% | 8.53% | 3.32% | 2.31% |
| 15min | 87.96% | 84.13% | 82.89% | 7.51% | 2.54% | 1.64% |
| 10min | 89.04% | 85.32% | 84.49% | 6.86% | 2.23% | 1.43% |
| 5min | 90.59% | 88.03% | 86.67% | 6.46% | 1.87% | 1.12% |
| 1min | 92.40% | 90.14% | 89.25% | 5.67% | 1.29% | 0.67% |
| 30sec | 93.22% | 91.00% | 90.02% | 5.45% | 1.35% | 0.71% |
| 15sec | 93.69% | 91.52% | 90.64% | 5.35% | 1.21% | 0.69% |

**Table 3:** Jump test: power and size. The table reports Monte Carlo simulations for the assessment of the power and size of the jump test. The empirical size and power of the jump test are computed at the 5%, 1%, and 0.5% theoretical size levels, respectively.

world. For this reason, the realized Amihud of SPY can be considered a good proxy for the overall liquidity condition on the equity market. As for the EUR/CHF and USD/CHF rates, our intent is to consider another financial security with different characteristics, for example, the OTC and dealership structure as well as a price setting for which it is not obvious to expect a (liquidity) leverage effect. The Swiss franc also provides us with an interesting laboratory, given that the peculiar behavior of both volume and volatility after the cap removal by the Swiss national bank in January 2015. This circumstance makes it an interesting case study for assessing the evolution of price impact measures around policy events that might change the structure of a financial market. The analysis of the stock market illiquidity is presented in Section 5.1, while Section 5.2 presents the results of the analysis conducted on the currency market.

| **Low Liquidity** | Power | | | Size | | |
|---|---|---|---|---|---|---|
| | 5% | 1% | 0.5% | 5% | 1% | 0.5% |
| 1h | 80.99% | 76.34% | 74.43% | 10.98% | 5.08% | 3.98% |
| 30min | 84.94% | 81.39% | 79.92% | 10.78% | 4.70% | 3.32% |
| 15min | 88.59% | 85.77% | 84.44% | 11.04% | 4.64% | 3.28% |
| 10min | 90.49% | 87.41% | 86.32% | 12.26% | 4.74% | 3.16% |
| 5min | 93.07% | 90.78% | 89.83% | 20.64% | 8.82% | 6.44% |
| 1min | 98.96% | 98.22% | 97.87% | 97.62% | 93.02% | 90.92% |
| 30sec | 99.70% | 99.45% | 99.32% | 100.00% | 100.00% | 100.00% |
| 15sec | 99.96% | 99.96% | 99.94% | 100.00% | 100.00% | 100.00% |
| **Medium Liquidity** | Power | | | Size | | |
| | 5% | 1% | 0.5% | 5% | 1% | 0.5% |
| 1h | 81.21% | 76.91% | 75.55% | 10.72% | 5.16% | 3.90% |
| 30min | 86.53% | 82.76% | 81.48% | 10.12% | 4.48% | 3.22% |
| 15min | 89.81% | 86.61% | 85.37% | 12.22% | 4.96% | 3.48% |
| 10min | 90.74% | 87.90% | 86.92% | 13.52% | 5.52% | 3.76% |
| 5min | 94.07% | 91.53% | 90.66% | 24.08% | 11.30% | 8.14% |
| 1min | 99.74% | 99.27% | 99.13% | 97.84% | 94.36% | 92.30% |
| 30sec | 100.00% | 99.94% | 99.92% | 100.00% | 100.00% | 99.98% |
| 15sec | 99.98% | 99.98% | 99.98% | 100.00% | 100.00% | 100.00% |
| **High Liquidity** | Power | | | Size | | |
| | 5% | 1% | 0.5% | 5% | 1% | 0.5% |
| 1h | 80.04% | 75.75% | 73.89% | 10.96% | 5.00% | 3.88% |
| 30min | 84.32% | 80.17% | 78.93% | 8.94% | 3.50% | 2.44% |
| 15min | 88.67% | 85.07% | 83.44% | 8.84% | 3.06% | 1.90% |
| 10min | 89.99% | 86.88% | 85.93% | 8.54% | 2.72% | 1.64% |
| 5min | 93.05% | 90.22% | 89.17% | 10.76% | 4.00% | 2.56% |
| 1min | 99.27% | 98.59% | 98.34% | 56.15% | 36.61% | 30.07% |
| 30sec | 99.70% | 99.62% | 99.54% | 97.88% | 92.80% | 89.72% |
| 15sec | 100.00% | 99.92% | 99.92% | 100.00% | 100.00% | 100.00% |

**Table 4:** Jump test: power and size with microstructure noise. The table reports Monte Carlo simulations for the assessment of the power and size of the jump test. The bid-ask spread is set at 0.15% relative to the price level. The empirical size and power of the jump test are computed at the 5%, 1%, and 0.5% theoretical size levels, respectively.

## 5.1 Illiquidity on the Equity Market

We consider the daily time series of the realized Amihud of SPY, which is computed as the ratio between the daily RPV obtained from intradaily returns sampled at different frequencies (source TAQ database) and the daily volume (expressed in dollars, source Bloomberg) on SPY for the period January 3, 2006, to June 29, 2018.

### 5.1.1 Sample Statistics

Table 5 reports the sample statistics of the RPV, volume, $\mathcal{A}$ (realized Amihud), $\mathcal{A}^C$ (its jump-robust version), and the jump-component of the realized Amihud, which is computed as $\mathcal{A}_t^{\mathcal{J}} = \frac{\mathbb{I}(\mathcal{J}>q_{1-\alpha})(RPV-\widetilde{MPV})}{v}$. The table also contains the sample statistics for the classic daily Amihud ($\mathcal{A}^D$) and of the high–low Amihud ($\mathcal{A}^{HL}$).[7] The series are computed using returns sampled at several frequencies (1, 5, 10, 15, and 30 minutes). In the last row, the table reports the number of significant jumps identified with the test in (9).

As expected, the variability of the realized Amihud is much smaller than that of the daily Amihud (by about 9 or 10 times), and this holds, irrespective of the sampling frequency used to compute the estimator. In turn, the variability of the $\mathcal{A}^{HL}$ is approximately three or four times lower than that of $\mathcal{A}^D$. All series display positive skewness and excess kurtosis compared with the reference value of the normal distribution. Interestingly, the kurtosis of the RPV is much larger than that of the realized Amihud. This suggests that RPV and trading volume tend to spike on the same days, so that dividing RPV by trading volume drastically reduces the observed kurtosis. Finally, volatility and volume are strongly correlated (around 85%); a somewhat expected result. However, the correlations of $\mathcal{A}$ with RPV and trading volume are smaller, about 22% and -28% (Pearson), signaling that liquidity interrelates with volatility and trading volumes, but still differs from them. The realized Amihud (computed with returns sampled at the 5-minute frequency) is positively correlated with both the daily and high–low Amihud. In particular, the correlation is much stronger with the latter, suggesting that $\mathcal{A}^{HL}$ is a more precise (or less noisy) measure of the illiquidity signal compared with $\mathcal{A}^D$.

### 5.1.2 Modeling Realized Amihud

Figure 4 displays the time series of the realized Amihud computed by employing returns sampled at the 5-minute frequency (black solid line), the daily Amihud (blue dotted line), and the high–low Amihud (yellow dashed line). Notably, the three series share very similar dynamic patterns, suggesting that they are all nonparametric measures of the same underlying stochastic quantity. However, the daily Amihud displays much more variability than the realized Amihud. Interestingly, the high–low Amihud, although being based on low-frequency data available at the daily horizon, displays a range of variability of an order close to that of the realized Amihud.

Looking at the time series features of the realized Amihud, its persistent nature can be seen. Indeed, it is evident that long periods with low illiquidity are followed by protracted periods of high illiquidity. Within the volatility literature, this is a well-established phenomenon known as *volatility clustering*. Because a similar pattern applies to the realized Amihud, we refer to it as *illiquidity clustering*. Figure 5 reports the empirical autocorrelation function (ACF) of the daily and realized Amihud. The realized Amihud displays strong persistence, as measured by the slow

[7] To interpret these measures as the amount of daily price volatility associated with one dollar of trading volume, in the empirical application, we multiply $\mathcal{A}^D$ by the constant $\sqrt{\pi/2}$ and $\mathcal{A}$ by the constant $\delta^{1/2}\sqrt{\pi/2}$. This guarantees that $\mathcal{A}$, $\mathcal{A}^D$, and $\mathcal{A}^{HL}$ are on the same scale.

| | Variance | | | | | |
|---|---|---|---|---|---|---|
| | 1min | 5min | 10min | 15min | 30min | Daily |
| RPV | 0.311 | 0.312 | 0.314 | 0.317 | 0.335 | 0.547 |
| Volume | – | – | – | – | – | 1.029 |
| $\mathcal{A}$ | 2.433 | 2.420 | 2.427 | 2.491 | 2.722 | – |
| $\mathcal{A}^{C}$ | 2.262 | 2.419 | 2.456 | 2.553 | 2.804 | – |
| $\mathcal{A}^{\mathcal{J}}$ | 0.053 | 0.030 | 0.042 | 0.063 | 0.149 | – |
| $\mathcal{A}^{D}$ | – | – | – | – | – | 9.541 |
| $\mathcal{A}^{HL}$ | – | – | – | – | – | 3.755 |
| | Skewness | | | | | |
| RPV | 3.871 | 3.650 | 3.700 | 3.820 | 3.824 | 3.476 |
| Volume | – | – | – | – | – | 1.984 |
| $\mathcal{A}$ | 1.306 | 1.294 | 1.200 | 1.152 | 1.038 | 1.245 |
| $\mathcal{A}^{C}$ | 1.203 | 1.277 | 1.184 | 1.139 | 0.963 | – |
| $\mathcal{A}^{\mathcal{J}}$ | 1.765 | 3.160 | 3.720 | 3.569 | 3.342 | – |
| $\mathcal{A}^{HL}$ | – | – | – | – | – | 1.453 |
| | Kurtosis | | | | | |
| RPV | 28.728 | 24.426 | 25.352 | 26.867 | 26.072 | 22.381 |
| Volume | – | – | – | – | – | 8.839 |
| $\mathcal{A}$ | 5.322 | 5.210 | 4.855 | 4.669 | 4.419 | 5.015 |
| $\mathcal{A}^{C}$ | 4.942 | 5.210 | 4.889 | 4.696 | 4.115 | – |
| $\mathcal{A}^{\mathcal{J}}$ | 7.741 | 13.490 | 18.639 | 18.161 | 16.162 | – |
| $\mathcal{A}^{HL}$ | – | – | – | – | – | 6.497 |
| # of significant jumps | 1896 | 386 | 314 | 343 | 413 | – |

| | Correlation Matrix | | | | | | |
|---|---|---|---|---|---|---|---|
| | RPV | Volume | $\mathcal{A}$ | $\mathcal{A}_t^{C}$ | $\mathcal{A}^{\mathcal{J}}$ | $\mathcal{A}^{D}$ | $\mathcal{A}^{HL}$ |
| RPV | – | 0.8860 | 0.2264 | 0.2377 | -0.1005 | 0.1171 | 0.1991 |
| Volume | 0.8470 | – | -0.1498 | -0.1356 | -0.1272 | 0.0374 | -0.0316 |
| $\mathcal{A}$ | 0.2200 | -0.2788 | – | 0.9937 | 0.0575 | 0.2250 | 0.6328 |
| $\mathcal{A}^{C}$ | 0.2375 | -0.2582 | 0.9906 | – | -0.0544 | 0.2198 | 0.6215 |
| $\mathcal{A}^{\mathcal{J}}$ | -0.1568 | -0.1267 | -0.0470 | -0.1680 | – | 0.0472 | 0.1015 |
| $\mathcal{A}^{D}$ | 0.1109 | 0.0239 | 0.1510 | 0.1443 | 0.0328 | – | 0.6662 |
| $\mathcal{A}^{HL}$ | 0.1830 | -0.1340 | 0.5997 | 0.5892 | 0.0171 | 0.5917 | – |

**Table 5:** Descriptive statistics. The table reports the sample statistics for the RPV, daily volume, the realized Amihud ($\mathcal{A}$), the Amihud's jump-robust version ($\mathcal{A}^{C}$), the jump component ($\mathcal{A}^{\mathcal{J}}$), the classic daily Amihud ($\mathcal{A}^{\mathcal{D}}$), the high–low Amihud ($\mathcal{A}^{\mathcal{HL}}$), as well as the number of significant jumps detected by the $\mathcal{J}$ test at the 1% significance level. The variance is scaled by a factor of E+04, while for the volume is scaled by a factor of E-16.. In the bottom panel, the table reports the Pearson–Spearman (upper/lower triangular matrix) correlations across the variables considered.

decay rate of the ACFs that remain very high even after 50 lags, whereas the autocorrelation of the daily Amihud is much less persistent. Concerning the daily Amihud, this is the typical behavior of persistent time series contaminated by additive noise, as indicated, for instance, by Hurvich and

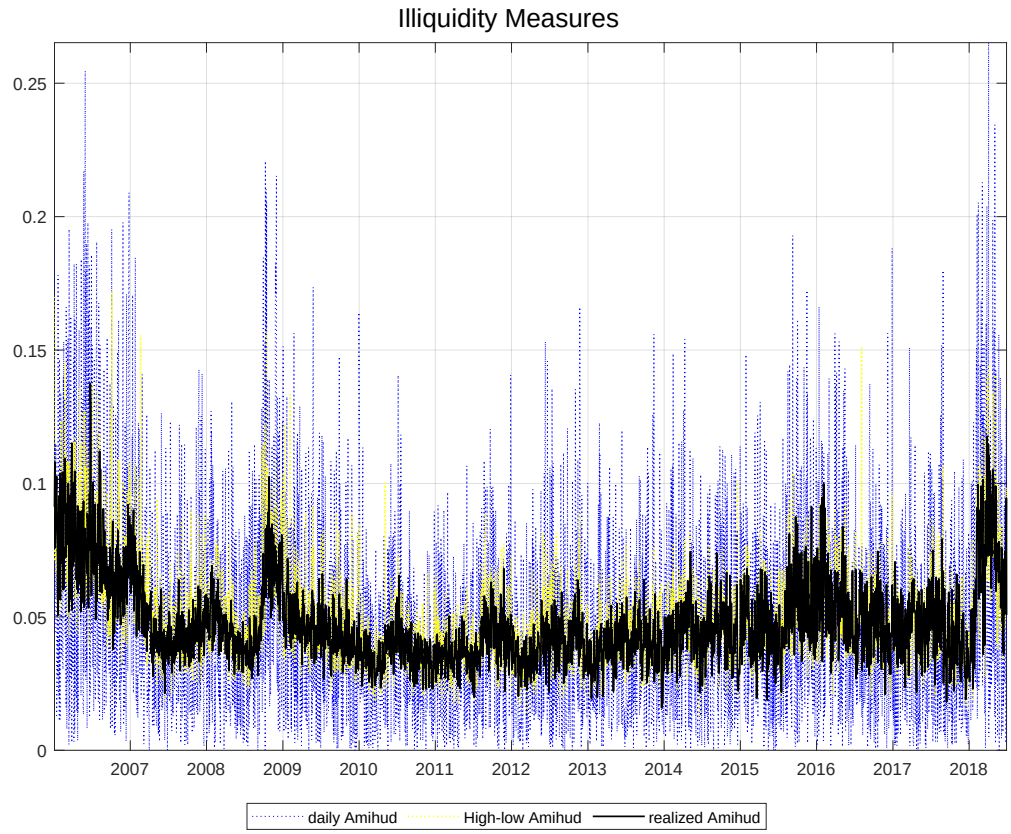


**Figure 4:** Illiquidity measurements. Realized Amihud (black solid line), daily Amihud (blue dotted line), and high–low Amihud (yellow dashed line) of SPY. Sample period: January 3, 2006 – June 29, 2018. Both series are scaled by a factor of E+09.

Ray (2003) and Hurvich et al. (2005) in the context of stochastic volatility estimation. Altogether, the evidence outlined in Figures 4 and 5 justifies the use of well-established volatility models for predicting illiquidity.

We consider both linear and nonlinear dynamic specifications for the realized Amihud. In particular, we consider a parametric model pertaining to the class of multiplicative error models (MEM) – as introduced by Engle (2002) and Engle and Gallo (2006). Inspired by the heterogenous autoregressive (HAR) model of Corsi (2009), we consider the MEM-AHAR model,[8] as follows

$$\mathcal{A}_t = \mu_t \epsilon_t, \tag{12}$$

where $\mu_t$ is the conditional mean of the process, and it follows asymmetric HAR dynamics as follows

$$\mu_t = \omega + \alpha_d \mathcal{A}_{t-1} + \alpha_w \bar{\mathcal{A}}_{w,t-1} + \alpha_m \bar{\mathcal{A}}_{m,t-1} + \gamma D_{t-1} \mathcal{A}_{t-1}, \tag{13}$$

where $\bar{\mathcal{A}}_{w,t-1} = \frac{1}{5}\sum_{i=1}^{5} \mathcal{A}_{t-i}$, $\bar{\mathcal{A}}_{m,t-1} = \frac{1}{22}\sum_{i=1}^{22} \mathcal{A}_{t-i}$, and $D_{t-1}$ is a dummy variable taking value of 1 if the return is negative and 0 otherwise; this accounts for an asymmetric response of illiquidity

[8] Appendix B reports a complete description of various alternative MEM and linear specifications, as well as their estimates on the sample under investigation.

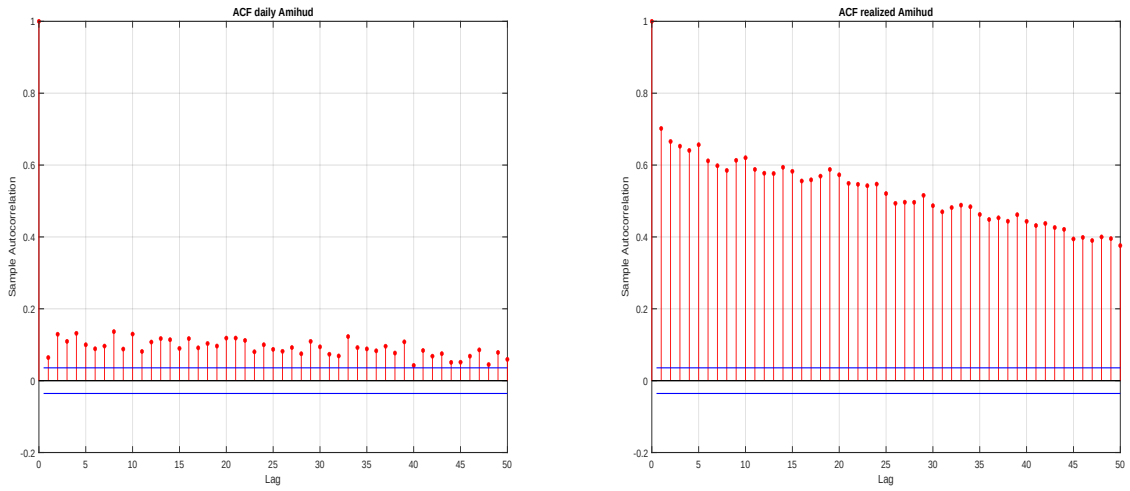


(a) Daily Amihud

(b) Realized Amihud

**Figure 5:** Autocorrelation. Empirical autocorrelation function of the daily Amihud (left panel) and of the realized Amihud (right panel).

to good or bad news. This is analogous to the GJR-GARCH(1,1) model by Glosten et al. (1993) that captures the illiquidity *leverage* effect. The term $\varepsilon_t$ denotes the innovation term, which is a non-negative random variable whose density is Gamma with a unit mean and variance equal to $\frac{1}{\vartheta}$. A sufficient condition for positivity of $\mu_t$ is that all coefficients in (13) are positive, while imposing $\alpha_d + \alpha_w + \alpha_m + \gamma/2 < 1$ ensures stationarity. Estimations are carried out using the maximum likelihood (ML), and we impose stationarity and positivity conditions upon estimating the models on the data.

Table 6 reports the estimation results of the MEM-AHAR model on the daily Amihud, high–low Amihud, and on the realized Amihud based on 5-minute returns (including the jump-robust version). Focusing on the last column of Panel a), the coefficients of $\mu_t$ for the realized Amihud are all positive and strongly significant at a 1% significance level, with a value of persistence around 93.6%, as measured by $\hat{\alpha}_d + \hat{\alpha}_w + \hat{\alpha}_m + \hat{\gamma}/2$. In the HAR framework, the coefficients $\alpha_d$, $\alpha_w$ and $\alpha_m$ summarize the impact trading at different frequencies, here induced by heterogeneity among market participants on market illiquidity. The results do not change when adopting the jump-robust realized Amihud. On the other hand, when noisier proxies of illiquidity are employed, such as in the daily Amihud or the high–low Amihud, the parameter associated with daily past illiquidity, that is, $\alpha_d$, is estimated on the lower bound, while the parameter $\alpha_w$ is significant only for the high–low Amihud. The only significant parameter is $\alpha_m$, indicating that a substantial smoothing is required on the daily Amihud to disentangle the expected illiquidity signal from its noisy ex-post measurement. Analogous evidence is found in the volatility literature when employing the realized GARCH model of Hansen et al. (2012) instead of the classic GARCH model on squared returns. In other words, the model assigns a small weight to the innovation term when the latter contains a substantial degree of measurement error. Furthermore, the implied persistence

| Panel a) | Estimation results | | | |
|---|---|---|---|---|
| | *Daily Amihud* | *High-Low Amihud* | *Jump-robust Amihud* | *Realized Amihud* |
| $\omega$ | $0.0160^a$ | $0.0052^a$ | $0.0030^a$ | $0.0029^a$ |
| | (0.0022) | (0.0011) | (0.0007) | (0.0007) |
| $\alpha_d$ | 0.0000 | 0.0000 | $0.1265^a$ | $0.1358^a$ |
| | (0.0234) | (0.0227) | (0.0225) | (0.0225) |
| $\alpha_w$ | 0.0011 | $0.3146^a$ | $0.3808^a$ | $0.3865^a$ |
| | (0.0494) | (0.0476) | (0.0401) | (0.0396) |
| $\alpha_m$ | $0.6595^a$ | $0.5549^a$ | $0.4087^a$ | $0.3983^a$ |
| | (0.0661) | (0.0466) | (0.0381) | (0.0373) |
| $\gamma$ | 0.0297 | $0.0546^a$ | $0.0399^a$ | $0.0371^a$ |
| | (0.0235) | (0.0103) | (0.0071) | (0.0069) |
| $\vartheta$ | $1.4608^a$ | $12.0371^a$ | $24.7189^a$ | $26.5139^a$ |
| | (0.0361) | (0.3188) | (0.5895) | (0.5591) |
| Panel b) | **Ljung-Box statistics (p–value)** | | | |
| LB(1) | 0.0045 | 0.2788 | 0.6561 | 0.7265 |
| LB(5) | 0.0453 | 0.0213 | 0.1608 | 0.2813 |
| LB(10) | 0.0714 | 0.0980 | 0.0001 | 0.0000 |

**Table 6:** MEM-AHAR estimated coefficients with robust standard errors (White, 1980) and $p$-value of the Ljung-Box statistics. Superscript *a, b* and *c* denote the 1%, 5%, and 10% significance levels, respectively. Sample period: January 3, 2006 – June 29, 2018.

obtained by the estimates of the MEM-AHAR coefficients on the daily and high-low Amihud is 67.5% and 89.7%, respectively. These values are much lower than those obtained on the realized Amihud, which is in line with the evidence of the ACFs reported in Figure 5. Finally, the estimate of $\vartheta$ (which is reciprocal of the variance of $\varepsilon$) for the daily Amihud is found to be around 16 times smaller than that of the realized Amihud. This implies that the variability of the innovation term is 16 times larger when employing the daily Amihud rather than the realized Amihud. This proportion is drastically reduced (approximately to half) when employing the high–low Amihud.

Overall, the results presented in Table 6 remain valid, even when alternative model specifications are employed; for more, see Tables 9 and 10 in Appendix B. In particular, the distribution of the innovation term seems to be well described by a Gamma distribution, while more sophisticated distributional choices[9] do not provide a remarkable improve in the fit.[10] This is due to the fact that the realized Amihud does not display extreme distributional features (see Table 5) because the ratio between volatility and volume drastically reduces the observed kurtosis. Finally, Panel b) of Table 6 reports the $p$-value for the Ljung-Box statistics. All model specifications cor-

[9] See the mixture MEM of Caporin et al. (2017) presented in Appendix B.1

[10] Figure 8 in the Appendix reports the probability-integral transform based on various MEM model specifications, here displaying a remarkable fit of the empirical distribution, even with simple MEM specifications.

rectly capture the persistent features of the series at hand because of the HAR-type specification for $\mu_t$; for instance, see Caporin et al. (2016, 2017).

### 5.1.3 Illiquidity and Stock Market Excess Returns

Following Amihud (2002), we carry out an analysis on the impact of illiquidity on stock market excess returns. As in Amihud (2002), the realized Amihud can be disentangled into two components: the *expected* illiquidity, as measured by the estimated conditional mean of the MEM-AHAR model, $\hat{\mu}_t$, and the *unexpected illiquidity*, as measured by the residual component $\hat{\epsilon}_t$. In particular, Table 7 reports the results of a simple regression analysis of the stock market excess returns (as measured by the difference between the returns of SPY and the risk free rate the U.S. 3-month treasury bills in our case) on illiquidity, that is:

$$r_t^e = \beta_0 + \beta_1 \mathcal{A}_t + u_t,$$

or on its components

$$r_t^e = \beta_0 + \beta_1 \hat{\mu}_t + \beta_2 \hat{\epsilon}_t + u_t.$$

| Panel a) | Total Illiquidity | | | | | | | | |
|---|---|---|---|---|---|---|---|---|---|
| | *Daily Amihud* | | | *High–Low Amihud* | | | *Realized Amihud* | | |
| | daily | weekly | monthly | daily | weekly | monthly | daily | weekly | monthly |
| Constant | 0.0363 | 0.0644 | 0.1515$^a$ | 0.0853 | 0.1016$^c$ | 0.1411$^b$ | 0.1747$^a$ | 0.1055$^b$ | 0.1337$^a$ |
| | (0.0359) | (0.0436) | (0.0492) | (0.0605) | (0.0530) | (0.0579) | (0.0489) | (0.0511) | (0.0510) |
| Illiquidity | -0.6747 | -1.2443 | −3.0133$^a$ | -1.6627 | −1.9886$^c$ | −2.7879$^b$ | −3.6736$^a$ | −2.1905$^c$ | −2.7951$^b$ |
| | (0.9147) | (1.0050) | (1.1137) | (1.3896) | (1.1566) | (1.2980) | (1.0687) | (1.1414) | (1.2282) |
| | Diagnostic | | | | | | | | |
| $R^2$ | 0.0007 | 0.0044 | 0.0533 | 0.0011 | 0.0056 | 0.0341 | 0.0034 | 0.0056 | 0.0314 |
| $R^2$ adj. | 0.0004 | 0.0028 | 0.0464 | 0.0008 | 0.0040 | 0.0271 | 0.0031 | 0.0040 | 0.0243 |
| F-test (p-value) | 0.2628 | 0.1865 | 0.0106 | 0.1195 | 0.1169 | 0.0521 | 0.0020 | 0.1165 | 0.0657 |
| Panel b) | Illiquidity decomposition | | | | | | | | |
| | *Daily Amihud* | | | *High–Low Amihud* | | | *Realized Amihud* | | |
| Constant | -0.0334 | 0.061 | -0.0184 | -0.0373 | 0.0471 | 0.0285 | -0.0731 | -0.0529 | −0.1612$^c$ |
| | (0.0877) | (0.0653) | (0.0720) | (0.0726) | (0.0550) | (0.0577) | (0.0710) | (0.0598) | (0.0917) |
| Expected Illiquidity | 0.7428 | -1.1749 | 0.4537 | 0.8171 | -0.8852 | -0.4951 | 1.66 | 1.241 | 3.6338$^c$ |
| | (1.8686) | (1.3687) | (1.5292) | (1.5508) | (1.1404) | (1.2079) | (1.6072) | (1.2600) | (1.8563) |
| Unexpected Illiquidity | -0.786 | -1.274 | −7.9535$^a$ | −3.1602$^c$ | −4.6013$^c$ | −17.0426$^a$ | −10.2752$^a$ | −14.0262$^a$ | −37.7907$^a$ |
| | (0.9224) | (1.1798) | (2.5456) | (1.7577) | (2.5736) | (6.0024) | (1.8958) | (5.0226) | (13.5283) |
| | Diagnostic | | | | | | | | |
| $R^2$ | 0.0010 | 0.0044 | 0.0821 | 0.0025 | 0.0084 | 0.0748 | 0.0107 | 0.0254 | 0.1619 |
| $R^2$ adj. | 0.0003 | 0.0012 | 0.0687 | 0.0019 | 0.0052 | 0.0613 | 0.0101 | 0.0223 | 0.1496 |
| F-test (p-value) | 0.6132 | 0.6884 | 0.0076 | 0.0536 | 0.2004 | 0.0132 | 0.0000 | 0.0010 | 0.0000 |

**Table 7:** Analysis regressing stock market excess returns on illiquidity measures (the top of the table) and on illiquidity decomposed into exepcted and unexpected components (the bottom of the table). The coefficients and Newey and West (1987) robust standard errors (in parenthesis) are multiplied by 100. Superscript *a*, *b* and *c* denote the 1%, 5%, and 10% levels of significance, respectively.

In Panel a), when employing the realized Amihud as the explanatory variable, the estimate of $\beta_1$ suggests that illiquidity is in a significantly negative relationship with the excess return. This holds true when aggregating at weekly and monthly (nonoverlapping) horizons. Notably, the $R^2$ turns out to be particularly large at the monthly horizon, being above 16%. Contrary to this, the relationship is less pronounced when employing the daily Amihud as the regressor. In particular, $\beta_1$ is not significant at the daily and weekly frequencies, but it is significant when the aggregation at monthly level is considered (in this case, the $R^2$ is around 5%). Again, this signals the fact that a less accurate measurement of illiquidity obtained via the daily Amihud masks the fundamental relationship between returns and illiquidity. This is confirmed by the analysis on the decomposed illiquidity in Panel b) of Table 7. Indeed, the expected illiquidity is never significant at the daily and weekly frequencies (irrespective of the measure adopted), while the *unexpected* illiquidity (as measured by the residuals of the MEM-AHAR model) is significantly and negatively related with excess returns when the realized Amihud and high–low Amihud are employed. Instead, the unexpected liquidity for the daily Amihud is only significant at the monthly horizon. This result squares well with the idea that the residual term of the MEM-AHAR model estimated on the daily Amihud is made of two components: the prediction error and the measurement error, where the latter seems to dominate at the daily and weekly frequencies.

## 5.2 Illiquidity on the Currency Market: the Swiss Franc Cap Removal

Another way to assess the general validity of the realized Amihud is by considering another financial instrument and using a meaningful episode, which is a sort of natural experiment. Through the lenses of the theory developed in Section 2, the announcement of the cap removal of the Swiss franc by the Swiss National Bank (SNB) on January 15, 2015, represents an ideal natural framework for conducting further testing. Starting from September 6, 2011, the SNB set a minimum exchange rate of 1.20 francs to the euro (capping the franc's appreciation), stating that "the value of the franc is a threat to the economy" and that it was "prepared to buy foreign currency in unlimited quantities." This means that the SNB had a declared binding *cap* on the transaction price that was removed on January 15, 2015.[11]

In terms of the trading model presented in Section 2, the SNB can be considered the special $(J+1)$-th trader. The SNB intervention strategy of selling CHF for EUR in potentially unlimited quantities would be implemented if the average of the reservation prices of the remaining $J$ traders ever fell below the cap, that is if $\frac{1}{J}\sum_{j=1}^{J} p^*_{i,j} < \log(1.2)$.[12] Indeed, despite the cap on the transaction price, the reservation prices of individual traders might well be below the 1.20 threshold. For instance, a trader with a reservation price of 1.12 (as the agent with the actual lowest forecast in Thomson Reuters survey before the SNB cap removal) is inclined to sell EUR for CHF.[13] In other

[11] The SNB announcement was somehow unanticipated by market participants; see, e.g., Jermann (2017) and Mirkov et al. (2016).

[12] There is empirical evidence that the SNB actually implemented this strategy by setting a huge ask volume (namely a *wall*) at 1.20; see Breedon et al. (2018, Figure 3, p.10).

[13] The Thomson Reuters survey indicates a wide dispersion of the beliefs of professional market participants around 1.20 for most of the capping period.

words, the SNB buys (sells) foreign (domestic) currency to guarantee that the transaction price is above the threshold, that is

$$p_i^{EUR|CHF} = \frac{1}{J+1}\sum_{j=1}^{J+1} p_{i,j}^{EUR|CHF,*} \geq \log(1.2), \tag{14}$$

where $p_{i,J+1}^{EUR|CHF,*} = \left(\log(1.2) - \frac{1}{J}\sum_{j=1}^{J} p_{i,j}^{EUR|CHF,*}\right) \times \mathbb{I}\left(\sum_{j=1}^{J} p_{i,j}^{EUR|CHF,*} < \log(1.2)\right)$, and $\mathbb{I}(\cdot)$ is the indicator function. The enforcement of the capping regime by the SNB generates extra trading volume. In particular, the trading volume is as follows

$$v_i^{EUR|CHF} = \frac{\lambda_i}{2}\sum_{j=1}^{J} |\Delta p_{i,j}^{EUR|CHF,*} - \frac{1}{J}\sum_{j=1}^{J} \Delta p_{i,j}^{EUR|CHF,*}| + v_i^{SNB}, \tag{15}$$

where $v_i^{SNB}$ is the trading volume generated by the central bank to maintain the cap on the FX rate. Hence, the model prescribes a low volatility of the observed returns because of the implicit constraint given by the capping and a larger volume because of the SNB interventions. This implies that the realized Amihud is lower (higher) before (after) the removal of the FX capping regime.

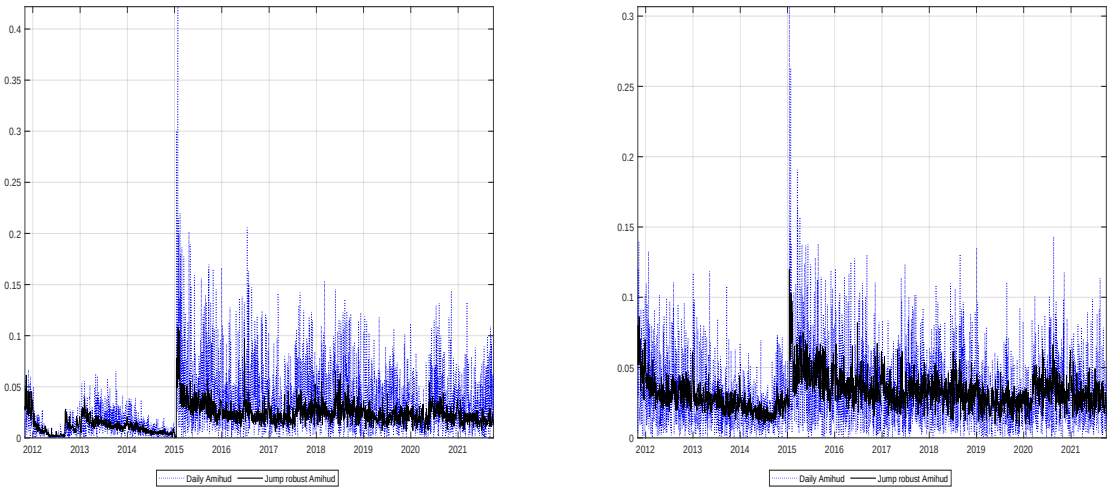


(a) EUR/CHF (b) USD/CHF

**Figure 6:** Daily Amihud (blue dotted lines, see Amihud, 2002) vs. the realized Amihud (black solid lines) of EUR/USD (Panel a) and USD/CHF (Panel b) exchange rates. Sample period: November 1, 2011 – September 30, 2021. Both series are scaled by a factor of E+11.

To empirically explore these model implications, we look at the daily time series of realized Amihud of the EUR/CHF and the USD/CHF FX spot rates covering the period November 1, 2011, to September 30, 2021. The time series are constructed from two distinct data sets. First, the CLS Group — the largest payment system for the settlement of foreign exchange transactions — provides us hourly data on the traded volume on both the EUR/CHF and USD/CHF rates. Second,

1-minute EUR/CHF and USD/CHF spot rates (bid, ask, high, low, and mid-quotes) are obtained from Olsen Financial Technologies. Given that trading on FX rates is active 24 hours a day, we consider the intradaily returns and volume solely between 8 a.m. and 8 p.m. (GMT time), thus limiting the influence of possible noisy observations associated with overnight hours in which there is minimal trading activity. Our final data set consists of 1, 943, 760 intradaily 1-minute returns and 32, 396 hourly trading volume for a total of 2, 492 trading days. Once again, we consider the returns sampled at both 5- and 10-minute frequencies to compute $RPV$ and $RPV_C$, while the daily volume is computed simply by aggregating the hourly volume.

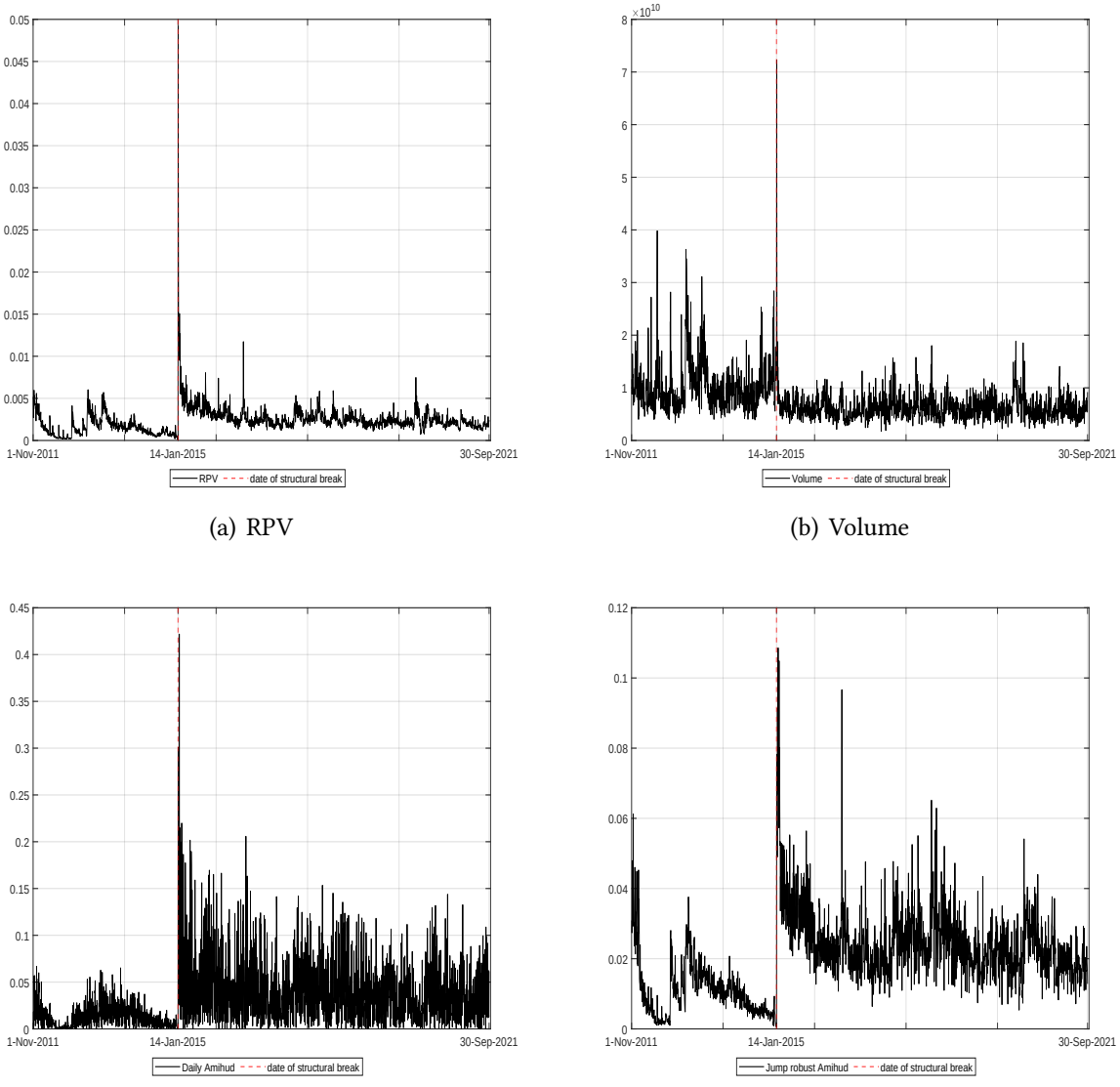


(a) RPV

(b) Volume

(c) Daily Amihud

(d) Realized Amihud

**Figure 7:** Break dates. The figures report the time series of RPV, volume, daily Amihud, and realized Amihud for the EUR/CHF rate (black solid line). The red vertical line denotes the break date, which is estimated by means of the Bai and Perron (1998) test for unknown break points. The test is performed with 15% trimming at the beginning and the end of the sample period and between break dates.

Figure 6 displays the time series of the realized Amihud (black solid lines) and daily Amihud

(blue dashed lines) of the EUR/USD (Panel a) and USD/CHF (Panel b) rates. As for SPY, the illiquidity clustering phenomenon is evident. High illiquidity characterizes the years after the onset of the sovereign debt crisis (in the period between 2010 and 2012). This period of stress greatly characterized the Swiss franc being considered a safe haven currency and giving it strong appreciation pressures (Jordan, 2020). On January 15, 2015, after the announcement by the SNB, we observe the highest peak of illiquidity, which remains very high for several months after this event. For both rates, Figure 6 reconfirms that the classic daily Amihud is much noisier than the corresponding realized version.

Figure 7 reports the result of Bai and Perron (1998)'s testing procedure to identify the date of a level break (if any) in a time series of RPV, volume, daily Amihud, and realized Amihud of EUR/CHF. The test considers the possible presence of one or more structural changes occurring at unknown dates: in particular, Bai and Perron (1998) propose a procedure designed to estimate the break dates, while testing for the presence of structural changes at the same time. We apply the Bai and Perron (1998) test with 15% trimming at the beginning and the end of the sample period and between the break dates (see also Casini and Perron, 2019, for a review and up-to-date recommendations about the procedure).[14] The series are characterized by strong persistence, and the procedure of Bai and Perron (1998) is robust to autocorrelation and heteroskedasticity. In all cases, the test identifies a significant break date on January 14, 2015, thus suggesting that the level of the series changes before and after this break date. The results for USD/CHF are reported in the Appendix and are analogous to those reported for EUR/CHF. In addition to significantly impacting a single currency pair, this result suggests that impotant events such as currency regime changes can affect commonality in the liquidity of financial securities.

**Estimation Results**

| | EUR/CHF | | | | USD/CHF | | | |
|---|---|---|---|---|---|---|---|---|
| | *Realized Amihud* | *RPV* | *Volume* | *Daily Amihud* | *Realized Amihud* | *RPV* | *Volume* | *Daily Amihud* |
| $const_1$ | $0.0109^a$ | $0.0016^a$ | $1.0159^a$ | $0.0129^a$ | $0.0279^a$ | $0.0039^a$ | $1.4617^a$ | $0.0300^a$ |
| | (0.0015) | (0.0002) | (0.0390) | (0.0008) | (0.0013) | (0.0002) | (0.0384) | (0.0010) |
| $const_2$ | $0.0248^a$ | $0.0027^a$ | $0.6205^a$ | $0.0422^a$ | $0.0345^a$ | $0.0038^a$ | $1.1315^a$ | $0.0352^a$ |
| | (0.0008) | (0.0001) | (0.0120) | (0.0010) | (0.0008) | (0.0001) | (0.0153) | (0.0007) |
| **Diagnostic** | | | | | | | | |
| $R^2$ | 0.3127 | 0.1009 | 0.2168 | 0.1638 | 0.0714 | 0.0004 | 0.1112 | 0.0076 |
| D-W statistics | 0.6384 | 0.6558 | 1.0136 | 1.7513 | 0.7912 | 0.9394 | 1.2655 | 1.8778 |

**Table 8:** Level estimation (robust standard errors in parenthesis) before and after the date January 14, 2015, for the EUR/CHF and USD/CHF FX rates. Superscripts *a*, *b*, and *c* denote the 1%, 5%, and 10% levels of significance, respectively. To account for heteroskedasticity and autocorrelation, the standard errors are computed based on the HAC estimator by following the automatic method in Andrews (1991) for the selection of the number of lagged autocovariances. Sample period: November 1, 2011 – September 30, 2021.

Table 8 reports the estimates of the mean of the series under investigation before and after the break date, which has been found on January 14, 2015. The results reported in the table strongly support the prescriptions of the theory. More specifically, the level of volatility (volume) significantly increases (decreases), thus leading to an increase of illiquidity (as measured by both daily

[14] We are grateful to Alessandro Casini for having shared with us the MATLAB codes for the break test.

and realized Amihud) on EUR/CHF. In a similar way, this shock also affects the other currency pair USD/CHF, which was not directly exposed to the capping on the EUR/CHF rate.

# 6 Conclusion

Liquidity is crucial to the well-functioning of financial markets and depends on how transaction volumes impact asset prices. A widely used measure to approximate this impact is the Amihud measure (Amihud, 2002). In the present paper, we have studied the theoretical and empirical properties of a refinement of the classic Amihud measure. We call it *realized Amihud* and it is defined as the ratio between the realized volatility and trading volume. Building on the simple trading mechanism introduced by Clark (1973), we develop the theory of realized volatility in the context of measuring market liquidity. Similar to the spot volatility, the instantaneous liquidity parameter, $\lambda$, is assumed to vary over time based on a dynamic process in continuous time; that is, liquidity is stochastic.

The result that clearly emerges from our study is that the *realized Amihud* provides a precise measurement of the inverse of *integrated liquidity*, that is, the integral $\mathcal{L} = \int_0^1 \lambda(s)ds$, over periods of fixed length (e.g., a day, a week, or a month). Because of its intrinsic nonparametric nature, the *realized Amihud* represents an alternative to well-known measures of illiquidity, which typically require the estimation of a parametric model. We propose another version in which price dispersion is measured by the high-low range. Its advantage is to be based on the highest and lowest prices achieved by a financial security during in certain time interval that are widely available even on a daily basis. Compared to the others, the range-based version is less accurate than the realized Amihud but more than the classic version. By employing the theory of multipower variation in Barndorff-Nielsen and Shephard (2003, 2004, 2006), we also provide a test statistic for detecting significant information jumps, which has good results in terms of both power and size (as seen in the results of the Monte Carlo simulations).

The empirical analysis based on more than a decade of representative data for the stock and currency markets illustrates the merits of the realized Amihud, unveiling features like illiquidity jumps, clustering and leverage effects. It also points to a sensible reduction of the noise in measuring illiquidity that might hide important structural relationships, such as that between illiquidity and excess returns.

# References

Abdi, F. and Ranaldo, A. (2017). A simple estimation of bid-ask spreads from daily close, high, and low prices. *Review of Financial Studies*, 30(12):4437–4480.

Amihud, Y. (2002). Illiquidity and stock returns: Cross-section and time-series effects. *Journal of Financial Markets*, 5:31–56.

Andersen, T. G. (1996). Return volatility and trading volume: An information flow interpretation of stochastic volatility. *The Journal of Finance*, 51(1):169–204.

Andersen, T. G. and Bollerslev, T. (1998). Answering the skeptics: Yes, standard volatility models do provide accurate forecasts. *International Economic Review*, 39(4):885–905.

Andersen, T. G., Bollerslev, T., Diebold, F. X., and Vega, C. (2007). Real-time price discovery in global stock, bond and foreign exchange markets. *Journal of International Economics*, 73(2):251–277.

Andrews, D. W. (1991). Heteroskedasticity and autocorrelation consistent covariance matrix estimation. *Econometrica: Journal of the Econometric Society*, pages 817–858.

Bai, J. and Perron, P. (1998). Estimating and testing linear models with multiple structural changes. *Econometrica*, pages 47–78.

Bandi, F. M., Kolokolov, A., Pirino, D., and Renò, R. (2020). Zeros. *Management Science*, 66(8):3466–3479.

Bandi, F. M. and Russell, J. R. (2008). Microstructure noise, realized variance, and optimal sampling. *The Review of Economic Studies*, 75(2):339–369.

Barndorff-Nielsen, O. E. and Shephard, N. (2002a). Econometric analysis of realized volatility and its use in estimating stochastic volatility models. *Journal of the Royal Statistical Society Series B*, 64:253–280.

Barndorff-Nielsen, O. E. and Shephard, N. (2002b). Estimating quadratic variation using realized variance. *Journal of Applied Econometrics*, 17(5):457–477.

Barndorff-Nielsen, O. E. and Shephard, N. (2003). Realized power variation and stochastic volatility models. *Bernoulli*, 9(2):243–265.

Barndorff-Nielsen, O. E. and Shephard, N. (2004). Power and bipower variation with stochastic volatility and jumps. *Journal of Financial Econometrics*, 2(1):1–37.

Barndorff-Nielsen, O. E. and Shephard, N. (2006). Econometrics of testing for jumps in financial economics using bipower variation. *Journal of Financial Econometrics*, 4(1):1–30.

Bauwens, L., Hafner, C. M., and Laurent, S. (2012). *Handbook of volatility models and their applications*, volume 3. John Wiley & Sons.

Bollerslev, T., Li, J., Xue, Y., et al. (2018). Volume, volatility and public news announcements. *The Review of Economic Studies*, 85(4):2005–2041.

Breedon, F., Chen, L., Ranaldo, A., and Vause, N. (2018). Judgement day: Algorithmic trading around the swiss franc cap removal. Technical report, Bank of England Working Paper.

Caporin, M., Rossi, E., and Santucci de Magistris, P. (2016). Volatility jumps and their economic determinants. *Journal of Financial Econometrics*, 14(1):29–80.

Caporin, M., Rossi, E., and Santucci de Magistris, P. (2017). Chasing volatility: A persistent multiplicative error model with jumps. *Journal of Econometrics*, 198(1):122–145.

Casini, A. and Perron, P. (2019). Structural breaks in time series. Oxford University Press.

Chaboud, A. P., Chernenko, S. V., and Wright, J. H. (2008). Trading activity and macroeconomic announcements in high-frequency exchange rate data. *Journal of the European Economic Association*, 6(2-3):589–596.

Chan, W. H. and Maheu, J. M. (2002). Conditional jump dynamics in stock market returns. *Journal of Business & Economic Statistics*, 20(3):377–389.

Christensen, K., Oomen, R. C., and Renò, R. (2022). The drift burst hypothesis. *Journal of Econometrics*, 227:461–497.

Clark, P. (1973). A subordinated stochastic process model with finite variance for speculative prices. *Econometrica: Journal of the Econometric Society*, 41(1):135–55.

Collin-Dufresne, P. and Fos, V. (2016). Insider trading, stochastic liquidity, and equilibrium prices. *Econometrica: Journal of the Econometric Society*, 84(4):1441–1475.

Corsi, F. (2009). A simple approximate long-memory model of realized volatility. *Journal of Financial Econometrics*, 7:174–196.

Corwin, S. A. and Schultz, P. H. (2012). A simple way to estimate bid-ask spreads from daily high and low prices. *Journal of Finance*, 67:719–759.

Engle, R. (2002). New frontiers for ARCH models. *Journal of Applied Econometrics*, 17(5):425–446.

Engle, R. F. and Gallo, G. M. (2006). A multiple indicators model for volatility using intra-daily data. *Journal of Econometrics*, 131(1-2):3–27.

Epps, T. W. and Epps, M. L. (1976). The stochastic dependence of security price changes and transaction volumes: Implications for the mixture-of-distributions hypothesis. *Econometrica: Journal of the Econometric Society*, pages 305–321.

Foucault, T., Pagano, M., and Röell, A. (2013). *Market Liquidity: Theory, Evidence, and Policy*. Oxford University Press.

Glosten, L. R., Jagannathan, R., and Runkle, D. E. (1993). On the relation between the expected value and the volatility of the nominal excess return on stocks. *The Journal of Finance*, 48(5):1779–1801.

Grossman, S. J. and Miller, M. H. (1988). Liquidity and market structure. *Journal of Finance*, 43(3):617–633.

Hansen, P. R., Huang, Z., and Shek, H. H. (2012). Realized GARCH: a joint model for returns and realized measures of volatility. *Journal of Applied Econometrics*, 27(6):877–906.

Hasbrouck, J. (2009). Trading costs and returns for us equities: Estimating effective costs from daily data. *The Journal of Finance*, 64(3):1445–1477.

Hurvich, C. M., Moulines, E., and Soulier, P. (2005). Estimating long memory in volatility. *Econometrica*, 73(4):1283–1328.

Hurvich, C. M. and Ray, B. K. (2003). The local Whittle estimator of long-memory stochastic volatility. *Journal of Financial Econometrics*, 1(3):445–470.

Jermann, U. J. (2017). Financial markets' views about the Euro-Swiss Franc floor. *Journal of Money, Credit and Banking*, 49:553–565.

Jiang, G. J., Lo, I., and Verdelhan, A. (2011). Information shocks, liquidity shocks, jumps, and price discovery: Evidence from the US treasury market. *Journal of Financial and Quantitative Analysis*, 46(2):527–551.

Jordan, T. (2020). Small country - big challenges: Switzerland's monetary policy response to the coronavirus pandemic. *2020 IMF Michel Camdessus Central Banking Lecture*, pages Washington and Zurich, 14.07.2020.

Karpoff, J. M. (1987). The relation between price changes and trading volume: A survey. *Journal of Financial and Quantitative Analysis*, 22(1):109–126.

Keynes, J. M. (1936). *The General Theory of Employment, Interest, and Money*. Palgrave Macmillan.

Kolokolov, A. and Renò, R. (2021). Jumps or staleness? *Available at SSRN 3882775*.

Kyle, A. S. (1985). Continuous auctions and insider trading. *Econometrica: Journal of the Econometric Society*, pages 1315–1335.

Lee, S. S. (2011). Jumps and information flow in financial markets. *The Review of Financial Studies*, 25(2):439–479.

Liu, L. Y., Patton, A. J., and Sheppard, K. (2015). Does anything beat 5-minute RV? A comparison of realized measures across multiple asset classes. *Journal of Econometrics*, 187(1):293–311.

Maheu, J. M. and McCurdy, T. H. (2004). News arrival, jump dynamics, and volatility components for individual stock returns. *The Journal of Finance*, 59(2):755–793.

Maheu, J. M., McCurdy, T. H., and Zhao, X. (2013). Do jumps contribute to the dynamics of the equity premium? *Journal of Financial Economics*, 110(2):457–477.

Mirkov, N., Pozdeev, I., and Soderlind, P. (2016). Toward removal of the Swiss franc cap: market expectations and verbal interventions. Working Paper Series 10/16, Swiss National Bank.

Müller, U. A., Dacorogna, M. M., Davé, R. D., Olsen, R. B., Pictet, O. V., and Von Weizsäcker, J. E. (1997). Volatilities of different time resolutions-analyzing the dynamics of market components. *Journal of Empirical Finance*, 4(2-3):213–239.

Newey, W. K. and West, K. D. (1987). A simple, positive semi-definite, heteroskedasticity and autocorrelation consistent covariance matrix. *Econometrica: Journal of the Econometric Society*, 55:703–708.

Parkinson, M. (1980). The extreme value method for estimating the variance of the rate of return. *Journal of Business*, 53:61–65.

Perraudin, W. and Vitale, P. (1996). Interdealer trade and information flows in a decentralized foreign exchange market. In Jeffrey A. Frankel, G. G. and Giovannini, A., editors, *The Microstructure of Foreign Exchange Markets*. University of Chicago Press.

Ranaldo, A. and Santucci de Magistris, P. (2022). Liquidity in the global currency market. *Journal of Financial Economics*, 146:859–883.

Roll, R. (1984). A simple implicit measure of the effective bid-ask spread in an efficient market. *The Journal of Finance*, 39:1127–1139.

Tauchen, G. E. and Pitts, M. (1983). The price variability-volume relationship on speculative markets. *Econometrica: Journal of the Econometric Society*, 51:485–505.

White, H. (1980). A heteroskedasticity-consistent covariance matrix estimator and a direct test for heteroskedasticity. *Econometrica: Journal of the Econometric Society*, pages 817–838.

# A Proofs

## A.1 Proof of Proposition 1

The proof of Proposition 1 proceeds as follows. By the properties of the super-position of independent processes, the limit for $\delta \to 0$ (or $I \to \infty$) of $RPV$ is as follows:

$$p \lim_{I\to\infty} \delta^{1/2} RPV = \sqrt{\frac{2}{\pi}}\mathcal{S}, \tag{16}$$

where $\mathcal{S} = \int_0^1 \overline{\sigma}(s)ds$ is the integrated average standard deviation and where the latter is defined as $\overline{\sigma}(t) = \frac{1}{J}\sqrt{\sum_{j=1}^{J} \sigma_j^2(t)}$. Indeed, similar to Barndorff-Nielsen and Shephard (2002b), $\Delta p_i = \frac{1}{J}\sum_{j=1}^{J} \Delta p_{i,j}^*$ is equivalent in law to $\int_{\delta(i-1)}^{\delta i} \overline{\sigma}(t)dW^*(t)$, where $\overline{\sigma}(t) = \frac{1}{J}\sqrt{\sum_{j=1}^{J} \sigma_j^2(t)}$. The aggregated volume on a unit (daily) interval is $v = \sum_{i=1}^{I} v_i$, and letting $I \to \infty$, we get

$$p \lim_{I\to\infty} \delta^{1/2} v = \frac{\mathcal{L}}{2}\sqrt{\frac{2}{\pi}}\overline{\mathcal{S}}, \tag{17}$$

with $\overline{\mathcal{S}} = \frac{1}{J}\sum_{j=1}^{J}\int_0^1 \varsigma_j(s)ds$, where $\varsigma_j(t) = \sqrt{(J-1)^2\sigma_j^2(t) + \sum_{s\neq j}\sigma_s^2(t)}$ and $\mathcal{L} = \int_0^1 \lambda(s)ds$ denotes the *integrated liquidity*. Hence, we get

$$p \lim_{I\to\infty} \mathcal{A} = \frac{2\mathcal{S}}{\mathcal{L}\overline{\mathcal{S}}}, \tag{18}$$

which reflects the ratio of the total average standard deviation carried by each trader. If $J = 2$, then $\overline{\mathcal{S}} = 2\mathcal{S}$, so that equation (5) in Proposition 1 follows directly, that is, $p\lim_{I\to\infty}\mathcal{A} = \frac{1}{\mathcal{L}}$.

Furthermore, by straightforward application of Barndorff-Nielsen and Shephard (2003, p.260), we get

$$\frac{\log\left(\sqrt{\pi\delta/2}\cdot RPV\right) - \log(\mathcal{S})}{\sqrt{\frac{\delta(\pi/2-1)RV}{(\pi\delta/2)RPV^2}}} \xrightarrow{d} N(0,1), \tag{19}$$

and

$$\frac{\log\left(\sqrt{\pi\delta/2}\cdot v\right) - \log(\mathcal{S}\mathcal{L})}{\sqrt{\frac{\delta(\pi/2-1)RV}{(\pi\delta/2)RPV^2}}} \xrightarrow{d} N(0,1). \tag{20}$$

where $RV$ is the realized variance and is defined as $RV^{=}\sum_{i=1}^{I}(r_i)^2$; for more, see, among others, Andersen and Bollerslev (1998). Following Barndorff-Nielsen and Shephard (2002a,b) and taking the limit for $\delta \to 0$ (i.e., $I \to \infty$), we get $p\lim_{I\to\infty} RV = \frac{1}{J^2}\mathcal{V}$, where $\mathcal{V} = \sum_{j=1}^{J}\mathcal{V}_j$ is the variation of the asset price on the unit interval generated by the aggregated individual components of $r$. The term $\mathcal{V}_j = \int_0^1 \sigma_j(s)^2 ds$ is the *integrated variance* associated with the $j$-th trader's specific component. By combining (19) and (20) and noticing that $\log(\mathcal{A}) = \log\left(\sqrt{\pi\delta/2}\cdot RPV\right) - \log\left(\sqrt{\pi\delta/2}\cdot v\right)$, the result in (6) follows. ■

## A.2 Traders homogeneity

Analogous results are obtained if $J \geq 2$ assuming homogeneity of traders, that is, $\sigma_j = \sigma \quad \forall j = 1, 2, \ldots, J$. In particular, the following proposition highlights the main determinants of the realized Amihud as an illiquidity measure under homogeneity of traders when $J \geq 2$.

**Proposition 2.** *Consider the illiquidity measure defined in (4), the equilibrium relation in (1), and the diffusive process for reservation prices in (2). Assume that $\sigma_j$ and $\lambda(t)$ are strictly positive càdlàg processes with (almost surely) square integrable sample paths with $\sigma_j(t) = \sigma(t)\ \forall j = 1, \ldots, J$. As $I \longrightarrow \infty$ (i.e., $\delta \longrightarrow 0$)*

$$p \lim_{I \to \infty} \mathcal{A} = \frac{2}{J\sqrt{J-1}\mathcal{L}}, \tag{21}$$

*Furthermore, as $I \longrightarrow \infty$*

$$\frac{\log(\mathcal{A}) - \log\left(\frac{2}{\mathcal{L}J\sqrt{(J-1)}}\right)}{\sqrt{\frac{J\delta(\pi/2-1)RV}{(J-1)(\pi\delta/2)RPV^2}}} \xrightarrow{d} N(0,1), \tag{22}$$

*where $RV^{=} \sum_{i=1}^{I} (r_i)^2$ is the realized variance.*

The proof of Proposition 2 follows the same steps as the proof of Proposition 1 in Section A.1. In this case, $\overline{\mathcal{S}} = J\sqrt{J-1}\mathcal{S}$, so that

$$p \lim_{I \to \infty} \mathcal{A} = \frac{2}{J\sqrt{J-1}\mathcal{L}}. \tag{23}$$

In this case, it follows that in the limit for $I \longrightarrow \infty$, the realized Amihud is inversely proportional to the integrated illiquidity and to the number of active traders in the market. By relaxing the assumption of homogeneity, $\mathcal{A}$ would converge in probability to the integrated illiquidity times the ratio of two measures of integrated volatility, namely $\frac{2\mathcal{S}}{\overline{\mathcal{S}}}$, that is, a weighted average of the price variability carried by each trader. Furthermore,

$$\frac{\log\left(\sqrt{\pi\delta/2} \cdot v\right) - \log\left(\mathcal{S}J\sqrt{J-1}\mathcal{L}\right)}{\sqrt{\frac{\delta(\pi/2-1)RV}{((J-1)\pi\delta/2)RPV^2}}} \xrightarrow{d} N(0,1), \tag{24}$$

so that

$$\frac{\log(\mathcal{A}) - \log\left(\frac{2}{\mathcal{L}J\sqrt{(J-1)}}\right)}{\sqrt{\frac{J\delta(\pi/2-1)RV}{(J-1)(\pi\delta/2)RPV^2}}} \xrightarrow{d} N(0,1). \tag{25}$$

■

# B Modeling Realized Amihud

In this section, we propose an econometric specification to characterize the dynamic evolution and distributional features of the realized Amihud. First, we consider parametric models belonging to the class of multiplicative error models (MEM), as introduced by Engle (2002) and Engle and Gallo (2006).

## B.1 A mixture MEM model

Following the same approach adopted by Caporin et al. (2017), it is possible to construct a MEM model featuring a component responsible for generating large and unexpected moves in illiquidity. In particular, following Caporin et al. (2017), we model $\mathcal{A}$ according to an AMEM with a mixture specification, namely AMEM-Mix. In the AMEM-Mix, $\mathcal{A}_t$ is given by the product of three elements:

$$\mathcal{A}_t = \mu_t Z_t \epsilon_t, \tag{26}$$

where $\mu_t$ is the conditional mean, and it follows asymmetric MEM (AMEM) dynamics:

$$\mu_t = \omega + \alpha \mathcal{A}_{t-1} + \beta \mu_{t-1} + \gamma D_{t-1} \mathcal{A}_{t-1}, \tag{27}$$

where $D_{t-1}$ is a dummy variable taking a value of 1 if the return is negative and 0 otherwise; it accounts for an asymmetric response of illiquidity to good or bad news. The term $\epsilon_t$ denotes the innovation term, whose density (conditional on the information set $\mathcal{F}_{t-1}$) is

$$f(\epsilon_t|\mathcal{F}_{t-1}) = \frac{1}{\Gamma(\vartheta)} \vartheta^{\vartheta} \epsilon_t^{\vartheta-1} e^{-\vartheta \epsilon_t}, \qquad \epsilon_t > 0, \quad \vartheta > 0. \tag{28}$$

This means that $\epsilon_t|\mathcal{F}_{t-1}$ is a gamma-distributed random variable with unit mean and variance equal to $\frac{1}{\vartheta}$. Finally, the mixing term, $Z_t$, is assumed to be independent of $\epsilon_t$ and distributed as a compound Poisson random variable

$$Z_t = \begin{cases} d_\kappa & N_t = 0, \\ \sum_{j=1}^{N_t} Y_{j,t} & N_t > 0, \end{cases} \tag{29}$$

where the expected number of arrivals at time $t$ ($N_t$) is governed by a Poisson random variable with a time-varying intensity, $\kappa_t$, and $d_\kappa$ is a positive function of $\kappa_t$ such that $E[Z_t \epsilon_t|\mathcal{F}_{t-1}] = 1$ and $E(\mathcal{A}|\mathcal{F}_{t-1}) = \mu_t$. Furthermore, $Y_{j,t}|\mathcal{F}_{t-1} \sim \Gamma(d_\kappa, \zeta)$. By the Poisson distribution, the probability of observing a $j \geq 0$, conditioning $\mathcal{F}_{t-1}$, is

$$Pr(N_t = j|\mathcal{F}_{t-1}) = \frac{e^{-\kappa_t} \kappa_t^j}{j!}, \qquad j = 0, 1, 2, \ldots. \tag{30}$$

Similar to Chan and Maheu (2002), we specify the dynamics of $\kappa_t$ as

$$\kappa_t = \phi_1 + \phi_2(\kappa_{t-1} - \phi_1) + \phi_3 \xi_{t-1}, \tag{31}$$

where the innovations, $\xi_t$, are defined as the error in predicting $N_t$ as new information becomes available in $\mathcal{F}_t$. In other words, $\xi_t = E(N_t|\mathcal{F}_t) - E(N_t|\mathcal{F}_{t-1})$, and in terms of model parameters

$$\xi_t = \sum_{j=0}^{\infty} jPr(N_t = j|\mathcal{F}_t) - \kappa_t. \tag{32}$$

The conditions $\phi_1 > 0$ and $1 > \phi_2 > \phi_3 > 0$ are sufficient to ensure positiveness and stationarity of $\kappa_t$, see Chan and Maheu (2002). A similar dynamics for the intensity has been adopted by Maheu and McCurdy (2004) and Maheu et al. (2013) for stock returns and by Caporin et al. (2016) for the realized variance. Finally, the filtered probability needed to compute $E(N_t|\mathcal{F}_t)$ is obtained via Bayes' rule, as follows:

$$Pr(N_t = j|\mathcal{F}_t) = \frac{f(\mathcal{A}_t|N_t = j, \mathcal{F}_{t-1})Pr(N_t = j|\mathcal{F}_{t-1})}{f(\mathcal{A}_t|\mathcal{F}_{t-1})}, \tag{33}$$

where the density of $\mathcal{A}_t$ conditional on $N_t = j$ and $\mathcal{F}_{t-1}$ is

$$f(\mathcal{A}_t|N_t = j, \mathcal{F}_{t-1}) = \begin{cases} \frac{1}{\mathcal{A}_t}\left(\frac{\vartheta \mathcal{A}_t}{d_\kappa \mu_t}\right)^{\vartheta} \frac{e^{\left(\frac{-\vartheta \mathcal{A}_t}{d_\kappa \mu_t}\right)}}{\Gamma(\vartheta)}, & N_t = 0 \\ \frac{2}{\mathcal{A}_t}\left(\frac{\mathcal{A}_t}{\mu_t}\frac{\vartheta\zeta}{d_\kappa}\right)\left(\frac{j\zeta+\vartheta}{2}\right)\frac{1}{\Gamma(j\zeta)\Gamma(\vartheta)}\mathbb{K}_{j\zeta-\vartheta}\left(2\sqrt{\frac{\mathcal{A}_t}{\mu_t}\frac{\vartheta\zeta}{d_\kappa}}\right), & N_t = j > 0, \end{cases} \tag{34}$$

where $\mathbb{K}(\cdot)$ is the modified Bessel function of a second kind, while the denominator in (33) is given by the following:

$$f(\mathcal{A}_t|\mathcal{F}_{t-1}) = e^{-\kappa_t} g_{\mathcal{A}_t} + \sum_{j=1}^{\infty} \frac{e^{-\kappa_t}\kappa_t^j}{j!} w_{\mathcal{A}_t}, \tag{35}$$

where $g_{\mathcal{A}_t}$ and $w_{\mathcal{A}_t}$ are $f(\mathcal{A}_t|N_t = j, \mathcal{F}_{t-1}, \alpha, \beta, \gamma)$ for $j = 0$ and $j > 0$, respectively. Therefore, the conditional density of $\mathcal{A}_t$ is a mixture of gamma and kappa distributions, whose weights are governed by the Poisson probabilities and by $\kappa_t$. The density is available in closed form, thus allowing us to estimate the model parameters by maximum likelihood. In the following analysis, we distinguish between the AMEM-Mix model with time-varying Poisson intensity (i.e., AMEM-Mix$_{\kappa_t}$) and with constant intensity (i.e., AMEM-Mix$_{\kappa}$), that is, $\kappa_t = \phi_1$.

## B.2 Estimation results

Table 9 reports the parameter estimates (and goodness of fit tests) for several AMEM and AMEM-Mix specifications estimated on daily and realized Amihud series of SPY, where the realized Amihud series is computed using returns sampled at 5- and 10-minute frequencies. Panel a) of Table 6 shows the coefficients from the specifications under consideration, which are all estimated using

maximum likelihood. As suggested by Engle and Gallo (2006), we allow $\mu_t$ to follow asymmetric GARCH-type or asymmetric HAR-type process with asymmetric response to negative returns. Panel b) of Table 6 displays the results of a number of diagnostics tests on the residuals and Poisson intensity innovations, that is, the $p$-values of the Ljung-Box test (at 1, 5, and 10, lags). Table 10 reports the parameter estimates of the linear and log-linear models. Looking at the estimates of the AMEM models in Table 9, we notice that the parameter $\alpha$ in the volatility literature is generally found in the range between 0.02 and 0.1 (Bauwens et al., 2012, ch. 1), while we find values in the range between 0.175 and 0.217 for the realized Amihud, signaling that illiquidity is more responsive to news than volatility. Instead, when the AMEM model is estimated on the daily Amihud, the estimates of $\alpha$ are significantly reduced because the daily Amihud is a more noisy proxy of the signal compared with the realized Amihud, so the model assigns a smaller weight to the parameter governing the news. Analogous evidence is found in the volatility literature when employing the realized GARCH model of Hansen et al. (2012) rather than a classic GARCH model on squared returns.

As for the parameter $\gamma$, it enters the model with the expected positive sign and is significant across all models, pointing at a more heavily reaction of illiquidity against negative returns rather than against positive returns. Altogether, by adopting the general view that uncertainty arises when new information reaches the market, we can state that illiquidity is strongly related to uncertainty among investors (as measured by volatility) and that this is responsible for the illiquidity persistence. Conversely, the estimates of the parameter $\beta$ is around 0.78 across models. This is in the lower bound of the interval of estimates of $\beta$ typically found for volatility (according to Bauwens et al., 2012, ch. 1, it is usually close to the upper limit of the interval 0.75–0.98). Finally, it is important to emphasize the behavior of the coefficient $\vartheta$ in the various AMEM and AMEM-Mix specifications, whose reciprocal is an estimate of the residuals variance. Notably, $\vartheta$ increases when moving from the simplest AMEM specifications to the sophisticated AMEM-Mix. Indeed, in the models with the mixtures, a significant part of the variability of the illiquidity is explained by mixture component $Z_t$. This finding testifies the need for a model that can assign the correct probability to large realizations of the illiquidity measure. As expected, the value of the log-likelihood function is larger for the AMEM-Mix specifications when compared with then simpler AMEM.

As for the Poisson intensity, the process $\kappa_t$ is very persistent ($\phi_2$ is around 0.998), signaling that the number of arrivals strongly depend on its past realizations.

| Panel a) | Estimation results | | | | | | | | | | | | | |
|---|---|---|---|---|---|---|---|---|---|---|---|---|---|---|
| | *Daily Amihud* | | *High–Low Amihud* | | *Realized Amihud - 5 minutes* | | | | | *Realized Amihud - 10 minutes* | | | | |
| | $AMEM-HAR$ | $AMEM(1,1)$ | $AMEM-HAR$ | $AMEM(1,1)$ | $AMEM-HAR$ | $AMEM(1,1)$ | $AMEM(2,1)$ | $AMEM(2,1)-Mix_k$ | $AMEM(2,1)-Mix_{k_t}$ | $AMEM-HAR$ | $AMEM(1,1)$ | $AMEM(2,1)$ | $AMEM(2,1)-Mix_k$ | $AMEM(2,1)-Mix_{k_t}$ |
| $\omega$ | 0.0160$^a$ | 0.0008$^a$ | 0.0052$^a$ | 0.0006$^a$ | 0.0030$^a$ | 0.0008$^a$ | 0.0008$^a$ | 0.0008$^a$ | 0.0008$^a$ | 0.0031$^a$ | 0.0008$^a$ | 0.0009$^a$ | 0.0008$^a$ | 0.0007$^a$ |
| | (0.0022) | (0.0003) | (0.0011) | (0.0002) | (0.0007) | (0.0002) | (0.0002) | (0.0002) | (0.0002) | (0.0007) | (0.0002) | (0.0002) | (0.0002) | (0.0002) |
| $\alpha_d$ | 0.0000 | 0.0176$^a$ | 0.0000 | 0.0759$^a$ | 0.1265$^a$ | 0.1752$^a$ | 0.2070$^a$ | 0.1978$^a$ | 0.2003$^a$ | 0.1252$^a$ | 0.1593$^a$ | 0.1955$^a$ | 0.1851$^a$ | 0.1848$^a$ |
| | (0.0234) | (0.0047) | (0.0227) | (0.0082) | (0.0225) | (0.0193) | (0.0180) | (0.0182) | (0.0181) | (0.0225) | (0.0183) | (0.0166) | (0.0165) | (0.0162) |
| $\alpha_w$ | 0.0011 | – | 0.3146$^a$ | – | 0.3808$^a$ | – | – | – | – | 0.3394$^a$ | – | – | – | – |
| | (0.0494) | – | (0.0476) | – | (0.0401) | – | – | – | – | (0.0417) | – | – | – | – |
| $\alpha_m$ | 0.6595$^a$ | – | 0.5549$^a$ | – | 0.4087$^a$ | – | – | – | – | 0.4432$^a$ | – | – | – | – |
| | (0.0661) | – | (0.0466) | – | (0.0381) | – | – | – | – | (0.0388) | – | – | – | – |
| $\beta_1$ | – | 0.9490$^a$ | – | 0.8938$^a$ | – | 0.7962$^a$ | 0.4494$^a$ | 0.4287$^a$ | 0.4174$^a$ | – | 0.8104$^a$ | 0.4088$^a$ | 0.3958$^a$ | 0.3958$^a$ |
| | – | (0.0100) | – | (0.0107) | – | (0.0219) | (0.0803) | (0.0842) | (0.0847) | – | (0.0213) | (0.0715) | (0.0715) | (0.0709) |
| $\beta_2$ | – | – | – | – | – | – | 0.3103$^a$ | 0.3393$^a$ | 0.3501$^a$ | – | – | 0.3588$^a$ | 0.3820$^a$ | 0.3850$^a$ |
| | – | – | – | – | – | – | (0.0746) | (0.0779) | (0.0784) | – | – | (0.0673) | (0.0673) | (0.0668) |
| $\gamma$ | 0.0297 | 0.0406$^a$ | 0.0546$^a$ | 0.0392$^a$ | 0.0399$^a$ | 0.0259$^a$ | 0.0329$^a$ | 0.0352$^a$ | 0.0347$^a$ | 0.0501$^a$ | 0.0299$^a$ | 0.0395$^a$ | 0.0413$^a$ | 0.0408$^a$ |
| | (0.0235) | (0.0101) | (0.0103) | (0.0053) | (0.0071) | (0.0042) | (0.0051) | (0.0051) | (0.0051) | (0.0072) | (0.0044) | (0.0054) | (0.0053) | (0.0053) |
| $\theta$ | 1.4608$^a$ | 1.4737$^a$ | 12.0371$^a$ | 12.1911$^a$ | 24.7189$^a$ | 24.2300$^a$ | 24.4870$^a$ | 26.1708$^a$ | 27.4063 | 21.91366$^a$ | 21.4118$^a$ | 21.6983$^a$ | 22.9429$^a$ | 24.3646$^a$ |
| | (0.0361) | (0.0364) | (0.3188) | (0.3146) | (0.5895) | (0.4910) | (0.5108) | (0.7786) | (0.5999) | (0.5023) | (0.5299) | (0.4806) | (0.5672) | (0.5847) |
| $\zeta$ | – | – | – | – | – | – | – | 9.2630$^a$ | 9.2251$^a$ | – | – | – | 7.3968$^a$ | 7.7027$^a$ |
| | – | – | – | – | – | – | – | (1.0397) | (0.6618) | – | – | – | (0.9656) | (0.8691) |
| $\phi_1$ | – | – | – | – | – | – | – | 0.0242$^b$ | 0.0226 | – | – | – | 0.0186$^a$ | 0.0186$^b$ |
| | – | – | – | – | – | – | – | (0.0109) | (0.0159) | – | – | – | (0.0071) | (0.0085) |
| $\phi_2$ | – | – | – | – | – | – | – | – | 0.9989$^a$ | – | – | – | – | 0.9986$^a$ |
| | – | – | – | – | – | – | – | – | (0.0006) | – | – | – | – | (0.0008) |
| $\phi_3$ | – | – | – | – | – | – | – | – | 0.0215$^a$ | – | – | – | – | 0.0248$^a$ |
| | – | – | – | – | – | – | – | – | (0.0046) | – | – | – | – | (0.0072) |
| LogLik | 6465.90 | 6517.19 | 9007.54 | 9080.08 | 10271.75 | 10296.32 | 10308.27 | 10318.59 | 10330.85 | 10114.51 | 10134.01 | 10150.41 | 10159.28 | 10176.26 |
| LRI | -0.0083 | -0.0163 | -0.0833 | -0.0920 | -0.1501 | -0.1528 | -0.1541 | -0.1553 | -0.1567 | -0.1385 | -0.1407 | -0.1425 | -0.1435 | -0.1454 |
| Panel b) | **Ljung-Box statistics (p–value)** | | | | | | | | | | | | | |
| Residuals: $\epsilon_t$ | | | | | | | | | | | | | | |
| LB 1 | 0.0045 | 0.0031 | 0.2788 | 0.5652 | 0.6561 | 0.0007 | 0.2836 | 0.2580 | 0.3039 | 0.6598 | 0.0001 | 0.2147 | 0.1231 | 0.1080 |
| LB 5 | 0.0453 | 0.0781 | 0.02132 | 0.0698 | 0.1608 | 0.0034 | 0.0835 | 0.0603 | 0.0599 | 0.2707 | 0.0013 | 0.1114 | 0.0706 | 0.0618 |
| LB 10 | 0.0714 | 0.0650 | 0.0980 | 0.0407 | 0.0001 | 0.0000 | 0.0000 | 0.0000 | 0.0000 | 0.0001 | 0.0000 | 0.0000 | 0.0000 | 0.0000 |
| Filtered Poisson innovations: $\xi_t$ | | | | | | | | | | | | | | |
| LB 1 | – | – | – | – | – | – | – | 0.1184 | 0.0400 | – | – | – | 0.3115 | 0.0945 |
| LB 5 | – | – | – | – | – | – | – | 0.0079 | 0.0056 | – | – | – | 0.0070 | 0.0000 |
| LB 10 | – | – | – | – | – | – | – | 0.0362 | 0.0188 | – | – | – | 0.0678 | 0.0000 |

**Table 9:** AMEM and mixture–AMEM estimated coefficients with robust standard errors (White, 1980) and $p$-value of the Ljung-Box statistics. Superscript $a$, $b$ and $c$ denote the 1%, 5%, and 10% significance levels, respectively. For the AMEM–Mix specification, we consider the model with constant jump intensity ($AMEM-Mix_\kappa$, i.e., $\phi_2 = \phi_3 = 0$) and with dynamic jump intensity ($AMEM - Mix_{\kappa_t}$). Sample period: January 3, 2006 – June 29, 2018.

## B.3 Linear specifications

We also consider linear specifications based on the HAR model of Corsi (2009). In particular, the linear asymmetric HAR (linear AHAR) model is given by

$$\mathcal{A}_t = \omega + \alpha_d \mathcal{A}_{t-1} + \alpha_w \bar{\mathcal{A}}_{w,t-1} + \alpha_m \bar{\mathcal{A}}_{m,t-1} + \gamma D_{t-1} \mathcal{A}_{t-1} + \varepsilon_t, \tag{36}$$

and the log-linear AHAR (log-linear AHAR) specification given by

$$\log \mathcal{A}_t = \omega + \alpha_d \log \mathcal{A}_{t-1} + \alpha_w \log \bar{\mathcal{A}}_{w,t-1} + \alpha_m \log \bar{\mathcal{A}}_{m,t-1} + \gamma D_{t-1} \log \mathcal{A}_{t-1} + \varepsilon_t, \tag{37}$$

| Panel a) | **Estimation results** | | | | | |
|---|---|---|---|---|---|---|
| | *Daily Amihud* | | *High–Low Amihud* | | *Realized Amihud* | |
| | Loglinear AHAR | Linear AHAR | Loglinear AHAR | Linear AHAR | Loglinear AHAR | Linear AHAR |
| $\omega$ | $-1.6182^a$ | $0.0148^a$ | $-0.3237^a$ | $0.0057^a$ | $-0.2024^a$ | $0.0027^a$ |
| | (0.2231) | (0.0025) | (0.0663) | (0.0015) | (0.0439) | (0.0006) |
| $\alpha_d$ | -0.0275 | $-0.0838^a$ | 0.0304 | -0.0152 | $0.1448^a$ | $0.1171^a$ |
| | (0.0227) | (0.0283) | (0.0207) | (0.0223) | (0.0259) | (0.0261) |
| $\alpha_w$ | 0.0406 | 0.0556 | $0.3313^a$ | $0.3534^a$ | $0.3711^a$ | $0.4208^a$\$ |
| | (0.0542) | (0.0575) | (0.0526) | (0.0576) | (0.0568) | (0.0730) |
| $\alpha_m$ | $0.5244^a$ | $0.7017^a$ | $0.5428^a$ | $0.5190^a$ | $0.4253^a$ | $0.3872^a$ |
| | (0.0845) | (0.0832) | (0.0496) | (0.0570) | (0.0513) | (0.0633) |
| $\gamma$ | $-0.0259^a$ | $0.0561^b$ | $-0.0210^a$ | $0.0565^a$ | $-0.0135^a$ | $0.0366^a$ |
| | (0.0100) | (0.0214) | (0.0032) | (0.0107) | (0.0024) | (0.0067) |
| Panel b) | **Ljung-Box statistics (p–value)** | | | | | |
| LB(1) | 0.9764 | 0.9260 | 0.5730 | 0.5507 | 0.5923 | 0.7050 |
| LB(5) | 0.8462 | 0.6273 | 0.2495 | 0.7036 | 0.0827 | 0.1768 |
| LB(10) | 0.4676 | 0.3781 | 0.0970 | 0.2749 | 0.0000 | 0.0000 |

**Table 10:** AHAR estimated coefficients with robust standard errors (White, 1980) and $p$-value of the Ljung-Box statistics. Superscript *a, b* and *c* denote the 1%, 5%, and 10% significance levels, respectively. Sample period: January 3, 2006 – June 29, 2018.

### B.3.1 PITs

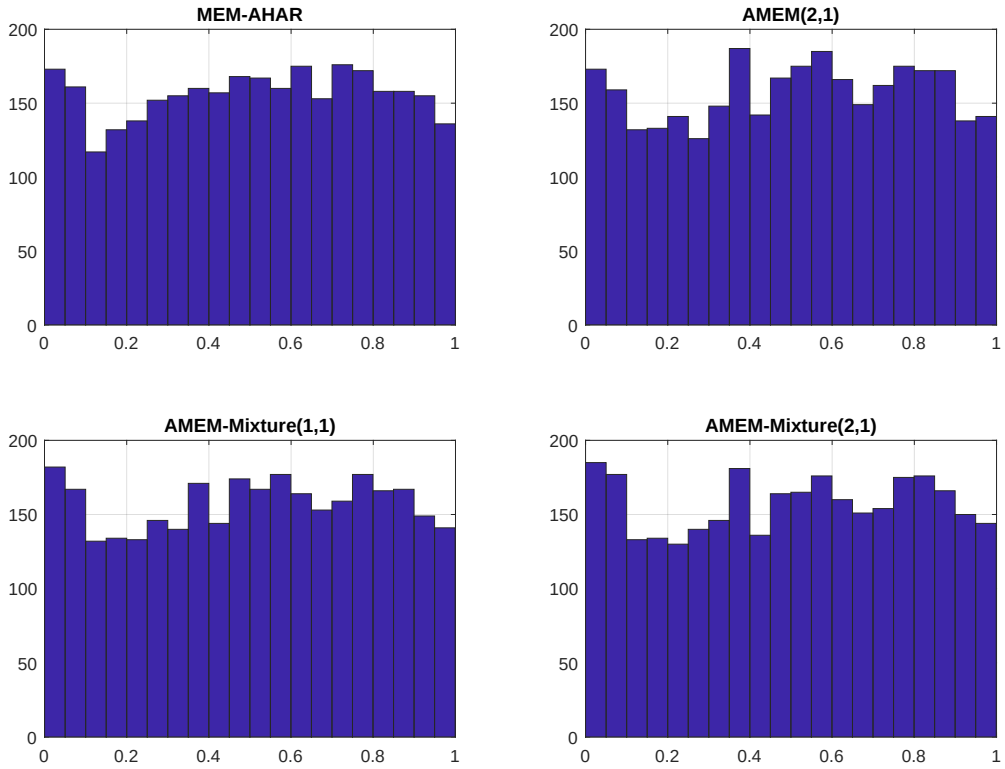


**Figure 8:** Probability integral transform (PIT) from MEM-HAR, AMEM(2,1) and mixture–AMEM . Sample period: January 3, 2006 – June 29, 2018.

## B.4 The USD/CHF analysis

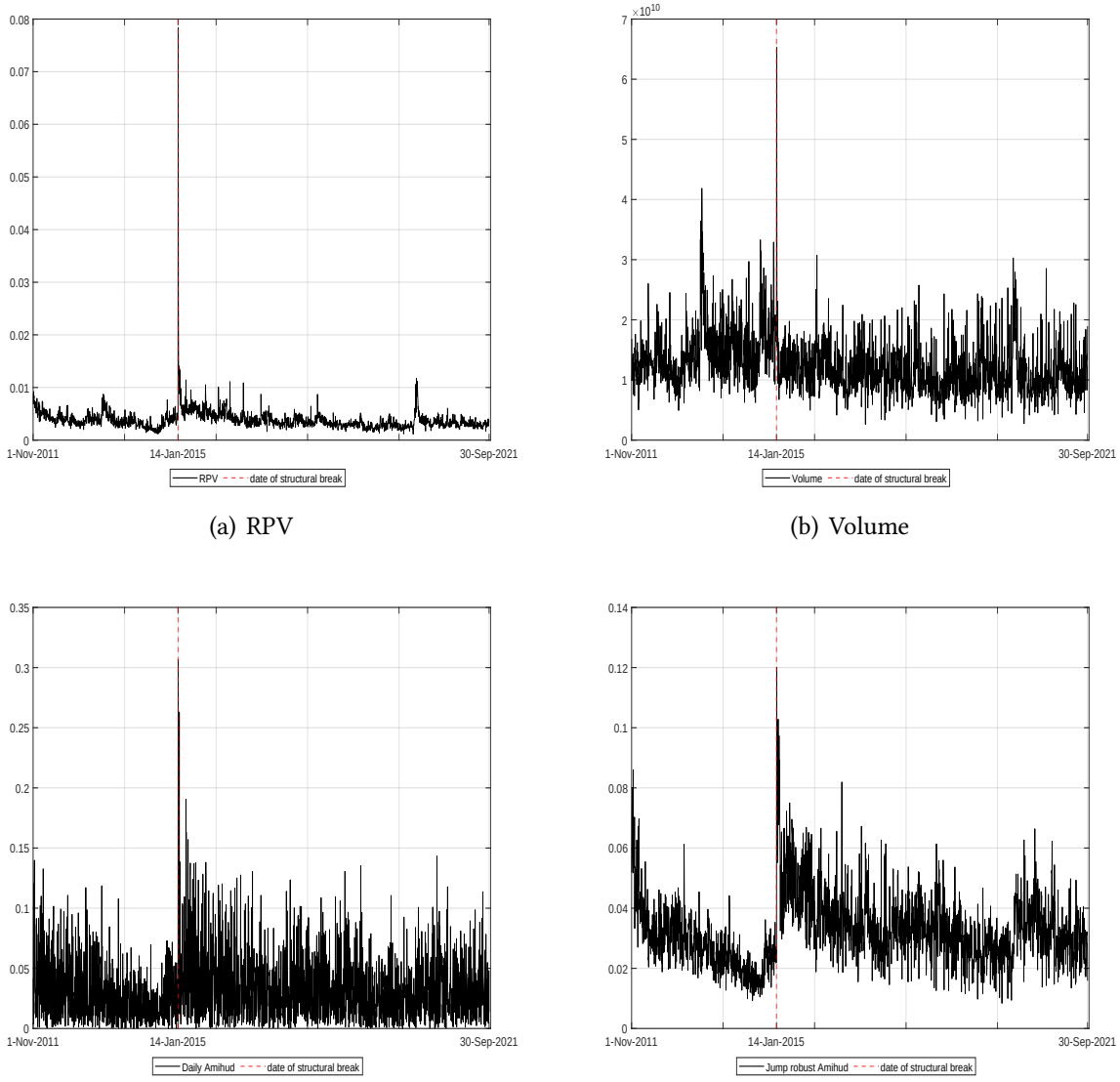


(a) RPV

(b) Volume

(c) Daily Amihud

(d) Realized Amihud

**Figure 9:** Break dates. The figures report the time series of RPV, volume, daily Amihud, and realized Amihud for the USD/CHF rate (black solid line). The red vertical line denotes the break date, which is estimated by means of the Bai and Perron (1998) test for unknown break points. The test is performed with 15% trimming at the beginning and the end of the sample period and between break dates.